



HAL
open science

One-sided variable sampling interval EWMA control charts for monitoring the multivariate coefficient of variation in the presence of measurement errors

Quoc-Thông T Nguyen, Vicent Giner-Bosch, Kim Duc Tran, Cédric Heuchenne, Kim Phuc Tran

► To cite this version:

Quoc-Thông T Nguyen, Vicent Giner-Bosch, Kim Duc Tran, Cédric Heuchenne, Kim Phuc Tran. One-sided variable sampling interval EWMA control charts for monitoring the multivariate coefficient of variation in the presence of measurement errors. *International Journal of Advanced Manufacturing Technology*, 2021, 115 (5-6), pp.1821-1851. 10.1007/s00170-021-07138-8 . hal-03544254

HAL Id: hal-03544254

<https://hal.science/hal-03544254v1>

Submitted on 8 Feb 2022

HAL is a multi-disciplinary open access archive for the deposit and dissemination of scientific research documents, whether they are published or not. The documents may come from teaching and research institutions in France or abroad, or from public or private research centers.

L'archive ouverte pluridisciplinaire **HAL**, est destinée au dépôt et à la diffusion de documents scientifiques de niveau recherche, publiés ou non, émanant des établissements d'enseignement et de recherche français ou étrangers, des laboratoires publics ou privés.

One-sided Variable Sampling Interval EWMA Control Charts for Monitoring the Multivariate Coefficient of Variation in the Presence of Measurement Errors

Quoc-Thông Nguyen · Vicent
Giner-Bosch · Kim Duc Tran · Cédric
Heuchenne · Kim Phuc Tran

Received: date / Accepted: date

Abstract Online monitoring of the multivariate coefficient of variation (MCV) can be of interest in many real situations in which the dispersion of a multivariate process is meant to remain constant with regards to its position. To this aim, several control charts have been recently proposed in the literature. In this paper, new one-sided adaptive charts to monitor the MCV are proposed. The chart applies a variable sampling interval (VSI) strategy on an exponentially weighted moving average (EWMA) scheme, aiming at benefiting from the known advantages of both approaches. Formulas to optimally determine the parameters of the chart are derived and presented. The proposed chart is shown to outperform competing charts under most circumstances. The presence of the measurement errors is considered to understand their effects on the charts. An illustrative example is also included.

Keywords Multivariate Coefficient of Variation · EWMA · Variable sampling interval · Average time to signal (ATS) · Measurement Errors.

Q. T. Nguyen

Institute of Artificial Intelligence and Data Science, Dong A University, Da Nang, Vietnam
HEC Management School, University of Liège, Liège 4000, Belgium
Université de Lille, ENSAIT, GEMTEX, F-59000 Lille, France

V. Giner-Bosch

Centre for Quality and Change Management, Universitat Politècnica de València, València, Spain

K. D. Tran

Institute of Artificial Intelligence and Data Science, Dong A University, Da Nang, Vietnam

C. Heuchenne

HEC Management School, University of Liège, Liège 4000, Belgium
E-mail: C.Heuchenne@uliege.be

K. P. Tran

Université de Lille, ENSAIT, GEMTEX, F-59000 Lille, France

1 Introduction

Statistical tools for quality control and improvement are a key element for companies and industry. Statistical process monitoring (SPM) provides practitioners with concrete instruments to ensure stability in production processes.

Quality has been sometimes defined as inversely proportional to variability [26]. From this point of view, it makes perfect sense the existence of control charts aimed at monitoring different variability measures of a process such as the range, the standard deviation or the coefficient of variation (CV). The (univariate) CV is defined as the quotient between the standard deviation and the mean. Because of this, it can be regarded as a relative measure of the dispersion of the quality characteristic of interest. In social sciences, the CV is also considered an *inequality* or *diversity* measure (see [2], for instance).

Because of its definition, monitoring the CV is useful in situations in which the dispersion of a process is meant to be kept constant with regards to its mean [16]. This is the case of different applications in engineering and in health, biological and social sciences, as reported in [40] and [18], among others. A considerable number of control charts for monitoring the CV have been developed, starting with the Shewhart-like one in [19], which has been later improved by other authors by adding different features such as adaptive and memory schemes [9, 41, 40, 44, 17]. See the recent work in [17] for a more complete review on this topic.

The CV-based approach has been also extended to a multivariate setting in the last years. The first (Shewhart-like) control chart for the multivariate CV (MCV) is due to [45]. Lim et al. [23] managed to improve the sensitivity of this first proposal by using a run-sum approach. Khatun et al. [20] adapted the Shewhart-like approach to short run processes, and Abbasi et al. [1] investigated the phase I. Khaw et al. [22] presented three adaptive charts for the MCV, while Khaw et al. [21] presented a synthetic chart. Haq et al. [18] and Giner-Bosch et al. [16] respectively developed an adaptive and a non-adaptive exponentially weighted moving average (EWMA) chart for the MCV. The synthetic approach was also investigated in [29]. Chew et al. [14] presented a new adaptive chart. Ng et al. [27] addressed the optimal design of control charts for the MCV from an economical perspective. Chew et al. [13] were the first in investigating run-rules charts for the MCV. Yet another adaptive chart for the MCV was presented in [30]. Chew et al. [11] investigated the run-rules scheme in short-run processes. Recently, Chew et al. [12] also researched into run rules for the MCV. Chew et al. [10] developed a new adaptive chart. Finally, Ayyoub et al. [3] studied the impact of measurement errors in the performance of Shewhart-like charts for the MCV. Since most of these papers were published within a short period of time, many of them do not refer to or include comparisons with each other. Suárez-Cabello et al. [38] used design of experiments (DOE) in order to examine the performance of the charts for the MCV presented in nine of the aforementioned papers [45, 23, 22, 21, 18, 16, 29, 14, 30]. It was found that the EWMA chart in [16] showed the best performance among the non-adaptive (i.e., fixed-parameter) charts being compared. Predictably,

this chart was found to be outperformed by the adaptive charts under consideration, with the exception of the variable-sampling-interval Shewhart-like chart in [30]. The variable-parameter chart in [14] was found to be the adaptive chart with the best performance. See [33] for further information on the use of DOE to calibrate or compare methods.

As already mentioned, adaptive charts usually result in better performance than non-adaptive ones, since the former offer more degrees of freedom and, thus, allow for better customisation than the latter. A control chart can be said to be *adaptive* if any of the parameters involved in its design is allowed to vary over time according to the current situation of the process [26, 39]. One of the possibilities is setting the time between consecutive samples free, which results in a so-called *variable-sampling-interval* (VSI) chart: basically, the sampling interval will be reduced if the process is more likely to be out of control, and will be increased when is more likely considered to be stable [39]. This idea was introduced for the first time in SPM in [32]. Interesting theoretical results regarding VSI charts have been developed in [32], [36], and [35], among others. Cui et al. [15] developed a VSI chart with run rules for the process mean. The first VSI cumulative sum (CUSUM) chart for the process mean was devised in [31]. The first VSI EWMA chart for the process mean is due to [37], who proved that their chart outperforms the non-adaptive EWMA and the VSI Shewhart-like charts, and outperforms the VSI CUSUM chart for small shifts. Yeong et al. [44] presented a VSI EWMA chart for the (univariate) CV, showing that it significantly outperforms other competing charts for the CV. A VSI EWMA distribution-free chart developed in [42] has been shown to be more efficient than the basic Arcsine EWMA Sign control chart.

The well-known EWMA scheme [34] manages to improve the sensitivity of Shewhart-like charts to detect process shifts —particularly, small ones [26]— by integrating information of past observations Y_0, Y_1, \dots, Y_{t-1} into each new observed value Y_t . It does so by computing and monitoring a weighted average Z_t of all present and past observations, recursively expressed as $Z_t = \lambda Y_t + (1 - \lambda)Z_{t-1}$.

In this paper, two one-sided VSI EWMA charts for the MCV are developed. This is expected to combine the advantages of the VSI and the EWMA approaches. Why did we choose the EWMA scheme to be the base of the VSI strategy? Because, as said before, it has been proven to be the most promising scheme for monitoring the MCV among the non-adaptive ones. Besides, despite some other adaptive strategies have been already proposed, a VSI EWMA can be regarded as a good compromise between simplicity and power. Moreover, the effect of the measurement error is also analysed for this VSI EWMA scheme. To the best of our knowledge, this adaptive scheme has not been previously addressed for the MCV including an evaluation of the effect of measurement error, and this is the reason why we are studying this impact in the present paper. Note that we will be using the same approach for modelling measurement error as other papers such as the one in [6] (see section 6), but this is the first time that this model is studied on a VSI EWMA chart for the MCV, as far as we are aware of. It is also important to note that in the study

on VSI EWMA for MCV, Ayyoub et al. [5] studied only the upward case due to the asymmetry of the distribution of the sample MCV.

The structure of the paper is organised as follows: a brief review of the distribution of the sample multivariate coefficient of variation squared is given in Section 2. The implementation of the VSI EWMA control charts for the multivariate CV squared is described in Section 3. The design of the optimal one-sided VSI EWMA control charts for the MCV is presented in Section 4. Section 5 discusses the performance of the proposed control charts without the measurement errors. Section 6 is devoted to describe the linear covariate error model for the MCV. The effect of the measurement errors is discussed in Section 7. An illustrative example is presented in Section 8, and some concluding remarks are given in Section 9.

2 The distribution of the sample multivariate coefficient of variation squared

We present, in this Section, an overview of the distribution of the sample multivariate coefficient of variation. Let us consider a random sample of size n , that is, $\mathbf{X}_1, \mathbf{X}_2, \dots, \mathbf{X}_n$ from a p -variate normal distribution with mean vector $\boldsymbol{\mu}$ and positive definite covariance matrix $\boldsymbol{\Sigma}$, i.e., $\mathbf{X}_i = (x_{i,1}, x_{i,2}, \dots, x_{i,p}) \sim N(\boldsymbol{\mu}, \boldsymbol{\Sigma})$, $i = 1, \dots, n$. According to [43], the multivariate CV is defined as

$$\gamma = (\boldsymbol{\mu}^T \boldsymbol{\Sigma}^{-1} \boldsymbol{\mu})^{-\frac{1}{2}}. \quad (1)$$

This definition is also used in [45] and [23]. Let $\bar{\mathbf{X}}$ and \mathbf{S} be the sample mean and the sample covariance matrix of $\mathbf{X}_1, \mathbf{X}_2, \dots, \mathbf{X}_n$, i.e.,

$$\bar{\mathbf{X}} = \frac{1}{n} \sum_{i=1}^n \mathbf{X}_i,$$

and

$$\mathbf{S} = \frac{1}{n-1} \sum_{i=1}^n (\mathbf{X}_i - \bar{\mathbf{X}})(\mathbf{X}_i - \bar{\mathbf{X}})^T.$$

Then, the sample multivariate coefficient of variation $\hat{\gamma}$ is defined as

$$\hat{\gamma} = (\bar{\mathbf{X}}^T \mathbf{S}^{-1} \bar{\mathbf{X}})^{-\frac{1}{2}}. \quad (2)$$

In a recent study, Giner-Bosch et al. [16] derived the cdf (cumulative distribution function) of $\hat{\gamma}^2$ based on [45] as

$$F_{\hat{\gamma}^2}(x | n, p, \gamma) = 1 - F_F\left(\frac{n(n-p)}{(n-1)px} \mid p, n-p, \frac{n}{\gamma^2}\right), \quad (3)$$

where $F_F(\cdot | p, n-p, n/\gamma^2)$ is the non-central F distribution with p and $n-p$ degrees of freedom and non-centrality parameter n/γ^2 .

3 Implementation of VSI EWMA- γ^2 control charts

In [30, 16], both VSI and EWMA schemes were developed to monitor the MCV. Our study investigates a scheme combining both EWMA and VSI schemes to improve the performance in monitoring the MCV. Two separated one-sided charts are proposed due to the skewness of the distribution of $\hat{\gamma}^2$, as specified in [29, 45]. We firstly recall the *fixed-sample-interval* (FSI) EWMA scheme for monitoring the MCV-squared as follow, for $i \geq 1$,

- To detect the increase in the MCV-squared, an upward EWMA control chart that monitors the following statistic is proposed:

$$Z_i^+ = \max(\mu_0(\hat{\gamma}^2), (1 - \lambda^+)Z_{i-1}^+ + \lambda^+\hat{\gamma}_i^2)$$

with the initial value $Z_0^+ = \mu_0(\hat{\gamma}^2)$, the corresponding lower control limit is $LCL^+ = \mu_0(\hat{\gamma}^2)$, and the upper control limit UCL^+ is defined as:

$$UCL^+ = \mu_0(\hat{\gamma}^2) + K_U \sqrt{\frac{\lambda}{2 - \lambda}} \sigma_0(\hat{\gamma}^2). \quad (4)$$

- To detect the decrease in the MCV-squared, a downward EWMA control chart that monitors the following statistic is proposed:

$$Z_i^- = \min(\mu_0(\hat{\gamma}^2), (1 - \lambda^-)Z_{i-1}^- + \lambda^-\hat{\gamma}_i^2)$$

with the initial value $Z_0^- = \mu_0(\hat{\gamma}^2)$, the corresponding upper control limit is $UCL^- = \mu_0(\hat{\gamma}^2)$, and the lower control limit LCL^- is defined as:

$$LCL^- = \mu_0(\hat{\gamma}^2) - K_D \sqrt{\frac{\lambda}{2 - \lambda}} \sigma_0(\hat{\gamma}^2) \quad (5)$$

The value of the computed MCV-squared in sample i , $\hat{\gamma}_i^2$, is calculated as in (2). In this definition, $\lambda^+ \in (0, 1]$ and $K_U > 1$, $\lambda^- \in (0, 1]$ and $K_D > 1$, are the smoothing and chart parameters of the upward, downward, chart, respectively. The process is initialised to the expected value of $\hat{\gamma}^2$, $\mu_0(\hat{\gamma}^2)$, when it is *in control* or *on target*, i.e., when the parameter γ is constant and equals an assumed value γ_0 , $\mu_0(\hat{\gamma}^2) = E(\hat{\gamma}^2|n, p, \gamma = \gamma_0)$. And $\sigma_0(\hat{\gamma}^2)$ is the standard deviation of $\hat{\gamma}^2$ when the process is *in control* or *on target*, $\sigma_0(\hat{\gamma}^2) = \sqrt{Var(\hat{\gamma}^2|n, p, \gamma = \gamma_0)}$. Analytical expressions to calculate both $\mu_0(\hat{\gamma}^2)$ and $\sigma_0(\hat{\gamma}^2)$ are provided in [16].

It is proven that the EWMA chart is sensitive to small and moderate shifts [26]. In comparison with others, however, it is less sensitive toward large shifts. The incorporation of the VSI feature into EWMA chart is then expected to improve this insensitivity toward large shifts and increase the performance of the charts in general. In the VSI EWMA- γ^2 control charts, the control limits UCL^+ and LCL^- are hold the same as those in original FSI charts. The difference is that the sampling interval, i.e., the time between two successive samples $\hat{\gamma}_i^2$ and $\hat{\gamma}_{i+1}^2$, is allowed to change based on the current value of Y_i^+ or Y_i^- . For the upward (downward) control chart, a longer sampling interval, h_L , is

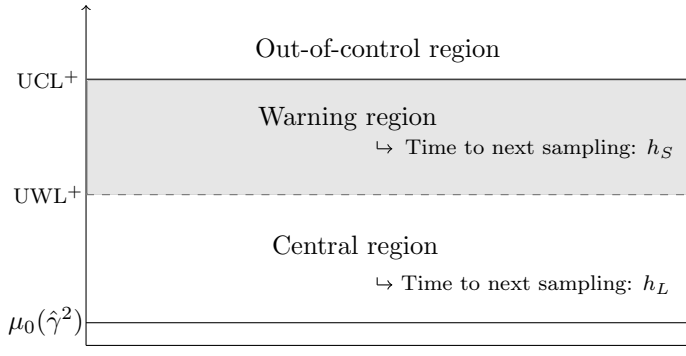


Fig. 1: Illustration of three regions of the upward VSI EWMA- γ^2 control charts.

used when the control statistic falls within central the region $[\mu_0(\hat{\gamma}^2), UWL^+]$ ($[LWL^-, \mu_0(\hat{\gamma}^2)]$), in which

$$UWL^+ = \mu_0(\hat{\gamma}^2) + W_U \sqrt{\frac{\lambda}{2-\lambda}} \sigma_0(\hat{\gamma}^2),$$

$$LWL^- = \mu_0(\hat{\gamma}^2) - W_D \sqrt{\frac{\lambda}{2-\lambda}} \sigma_0(\hat{\gamma}^2),$$

with UWL^+ is the upper warning limit of the upward chart, and LWL^- is the lower warning limit of the downward chart. The short sampling interval, h_S , is applied when the monitored statistic falls within the warning region $[UWL^+, UCL^+]$ in upward case, or $[LCL^-, LWL^-]$ in downward case. An out-of-control signal is given at time i if $Z_i^+ > UCL^+$ for the upward chart, or $Z_i^- < LCL^-$ for the downward chart. Thus, in VSI EWMA scheme, the control interval is separated into three regions: the central region, the warning region, and the out-of-control region. A graphical view of the operation of an upward VSI EWMA- γ^2 control chart is illustrated in Figure 1. The warning limit UWL^+ for upward chart and LWL^- for downward chart are defined through the new parameters called the warning limit coefficients, $0 < W_U < K_U$ and $0 < W_D < K_D$. They represent the relation between the warning region and the safe region in the sense that when the value of W_U or W_D is smaller, the central region is narrower compared with the warning region.

4 Design of optimal VSI EWMA- γ^2 control charts

We first present a method to compute the average time to signal (ATS) for the two one-sided VSI EWMA- γ^2 control charts. The *ATS* measures the expected time before the control chart signals an ‘out-of-control alarm’ after the

occurrence of an assignable cause or the issue of a false alarm. When a process is in-control (i.e., when $\gamma = \gamma_0$), the average time for the chart to signal a false alarm is denoted by ATS_0 ; otherwise, when there is a real shift in the process (i.e., when $\gamma = \gamma_1 \neq \gamma_0$), the average time for the chart to rise an alarm is denoted by ATS_1 . The size of the shift is usually denoted by

$$\tau = \frac{\gamma_1}{\gamma_0}. \quad (6)$$

By its meaning, it is desirable to design a chart with smaller ATS_1 while the ATS_0 is still the same in comparison with others. For a FSI model, the ATS is a multiple of the ARL and the fixed sampling interval h_F , namely,

$$ATS^{\text{FSI}} = h_F \times ARL^{\text{FSI}}. \quad (7)$$

For a VSI model, the ATS is computed as:

$$ATS^{\text{VSI}} = E(h) \times ARL^{\text{VSI}}, \quad (8)$$

where $E(h)$ is the average of sampling interval time.

The ATS measure is approximated using the discrete Markov chain approach proposed in [7]. In this method, we partition the control interval into a set of s subintervals corresponding to $s+2$ states of the Markov chain. The more number of subintervals s is, the better the approximation to the original continuous setting is. The width of each subinterval is 2δ where $\delta = \frac{UCL^+ - \mu_0(\hat{\sigma}^2)}{2s}$ for the upward chart, $\delta = \frac{\mu_0(\hat{\sigma}^2) - LCL^-}{2s}$ for the downward chart. The value of s is chosen so that each midpoint H_j , $j = 1, \dots, s$ can be considered as the representative of the sub-interval $(H_j - \delta, H_j + \delta]$. Figure 2 illustrates the subdivision of the in-control range for an upward chart.

Among the $s+2$ states of the Markov chain, the state 0 corresponds to the line H_0 , the in-control transient state j corresponds to the j^{th} sub-intervals, $j = 1, \dots, s$, while the state $s+2$ presents out-of-control or absorbing state. If the statistic Z_i^+ or Z_i^- fall into a sub-interval j , the Markov chain is in the transient state j for sample i^{th} ; if not, the process reaches absorbing state. The transition probability matrix \mathbf{P} of this discrete Markov chain is

$$\mathbf{P} = \begin{pmatrix} \mathbf{Q} & \mathbf{r} \\ \mathbf{0}^T & \mathbf{1} \end{pmatrix} = \begin{pmatrix} Q_{0,0} & Q_{0,1} & \dots & Q_{0,s} & r_0 \\ Q_{1,0} & Q_{1,1} & \dots & Q_{1,s} & r_1 \\ \vdots & \vdots & & \vdots & \\ Q_{s,0} & Q_{s,1} & \dots & Q_{s,s} & r_s \\ 0 & 0 & \dots & 0 & 1 \end{pmatrix}.$$

In this formula, \mathbf{Q} is the $(s+1, s+1)$ matrix of transient probabilities, $\mathbf{0} = (0, 0, \dots, 0)^T$ and the $(s+1)$ vector \mathbf{r} satisfies $\mathbf{r} = (\mathbf{1} - \mathbf{Q}\mathbf{1})$ (row probabilities must sum to 1) with $\mathbf{1} = (1, 1, \dots, 1)^T$. Denote \mathbf{q} the $(s+1, 1)$ vector of initial probabilities associated with the $p+1$ transient states, i.e., $\mathbf{q} = (q_0, q_1, \dots, q_s)^T$. The transient probability $Q_{i,j}$, $i = 0, 1, \dots, s$, of the matrix \mathbf{Q} is defined by

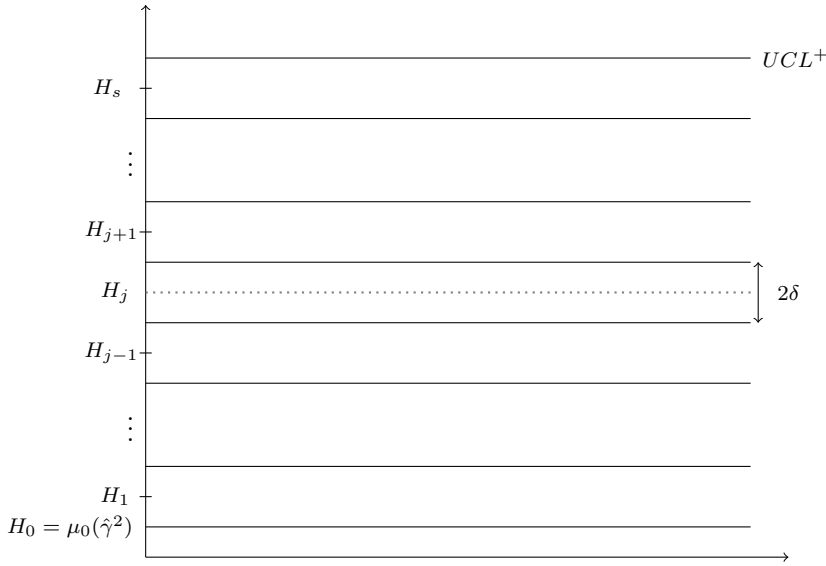


Fig. 2: Subdivision of the in-control range into s equally spaced subintervals of width 2δ .

– if $j = 0$,

$$\text{for the upward chart : } Q_{i,0} = F_{\hat{\gamma}_i^2} \left(\frac{\mu_0(\hat{\gamma}^2) - (1-\lambda^+)H_i}{\lambda^+} \middle| p, n-p, \gamma \right),$$

$$\text{for the downward chart : } Q_{i,0} = 1 - F_{\hat{\gamma}_i^2} \left(\frac{\mu_0(\hat{\gamma}^2) - (1-\lambda^-)H_i}{\lambda^-} \middle| p, n-p, \gamma \right);$$

– if $j = 1, 2, \dots, p$, for both upward and downward charts,

$$Q_{i,j} = F_{\hat{\gamma}_i^2} \left(\frac{H_j + \delta - (1-\lambda)H_i}{\lambda} \middle| p, n-p, \gamma \right) - F_{\hat{\gamma}_i^2} \left(\frac{H_j - \delta - (1-\lambda)H_i}{\lambda} \middle| p, n-p, \gamma \right),$$

where $F_{\hat{\gamma}_i^2}(\cdot)$ is the cdf of $\hat{\gamma}_i^2$ as defined in (3) while λ is either λ^+ or λ^- , corresponding to upward or downward case. The vector \mathbf{q} of initial probabilities, concerning the zero-state condition, equal $\mathbf{q} = (1, 0, \dots, 0)$. As introduced in [7], and reproduced in [24], the *ATS* is calculated as follows:

$$ATS = \mathbf{q}^T (\mathbf{I} - \mathbf{Q})^{-1} \mathbf{g} \quad (9)$$

where \mathbf{I} is the $s \times s$ identity matrix, \mathbf{g} is the vector of sampling intervals corresponding to the states of the Markov chain. The element g_j of the vector

\mathbf{g} is the sampling interval when the control statistic is in the state j ,

$$g_j = \begin{cases} h_S & \text{if } H_j \in [UWL^+, UCL^+] \text{ or } H_j \in [LCL^-, LWL^-] \\ h_L & \text{if } H_j \in [\mu_0(\hat{\gamma}^2), UWL^+] \text{ or } H_j \in [LWL^-, \mu_0(\hat{\gamma}^2)]. \end{cases} \quad (10)$$

From (8) and (9), the expected sampling interval $E(h)$ can be deduced as:

$$E(h) = \frac{\mathbf{q}^T(\mathbf{I} - \mathbf{Q})^{-1}\mathbf{g}}{\mathbf{q}^T(\mathbf{I} - \mathbf{Q})^{-1}\mathbf{1}}, \quad (11)$$

the denominator in (11) is the formula for ARL as in [7].

Without loss of generality, in this paper, it is assumed that the constant sampling interval in FSI control charts is supposed to be time unit, i.e. $h_F = 1$, which leads to $ATS_0^{FSI} = ARL_0$ by plugging h_F into (7). For the sake of comparison between the two types of control charts (FSI and VSI), when the process is in-control, the constraints are made the same for both average time to signal ATS_0 and average sampling interval $E_0(h)$. Lucas et al. [24] suggested that it is optimal to use two sampling intervals for detecting a specified shift of the process target value. As proposed in [44, 8], A fixed couple (h_S, h_L) is typically chosen for a VSI scheme. Since h_S represents the shortest feasible time interval between subgroups from the process, it is reasonable to fix the value of h_S according to the manufacturing conditions. However, it is more practical if the value of h_L is considered by the scheme. Once the control statistic is in central region, the process is still in the safe state and the next sampling interval can be chosen freely as long as it does not affect the performance of the chart. Therefore, we propose to have the warning limit coefficient $W_U(W_D)$ fixed instead of the value of h_L . The optimal parameters to estimate now are (λ^+, K_U, h_L) for upward chart, and (λ^-, K_D, h_L) for downward chart, using fixed values of h_S . For a given shift size τ , we estimate the combination $(\lambda^{+*}, K_U^*, h_L^*)$ or $(\lambda^{-*}, K_D^*, h_L^*)$ such that

– for upward chart,

$$(\lambda^{+*}, K_U^*, h_L^*) = \arg \min_{(\lambda^+, K_U, h_L)} ATS(n, \lambda^+, K_U, W_U, \gamma_0, p, \tau, h_L, h_S) \quad (12)$$

subject to the constraint

$$\begin{cases} ATS(n, \lambda^{+*}, K_U^*, W_U, \gamma_0, p, \tau = 1, h_L^*, h_S) = ATS_0 \\ E_0(h) = 1; \end{cases}$$

– for downward chart,

$$(\lambda^{-*}, K_D^*, h_L^*) = \arg \min_{(\lambda^-, K_D, h_L)} ATS(n, \lambda^-, K_D, W_D, \gamma_0, p, \tau, h_L, h_S) \quad (13)$$

subject to the constraint

$$\begin{cases} ATS(n, \lambda^{-*}, K_D^*, W_D, \gamma_0, p, \tau = 1, h_L^*, h_S) = ATS_0 \\ E_0(h) = 1. \end{cases}$$

5 Numerical performance one-sided VSI EWMA MCV control charts without the presence of measurement errors

In this Section, we present the numerical results to evaluate the performance of both upward and downward VSI EWMA- γ^2 control charts. The problems (12), (13) are solved to find the optimal parameters that minimise ATS subjecting to the corresponding constraints. For the sake of comparison, the ATS_0 is set to 370.4 and $E_0(h) = 1$. The optimisation solving is implemented with Matlab using Levenberg–Marquardt algorithm [25] based on a number of following scenarios of parameters:

- $\gamma_0 \in \{0.1, 0.2, 0.3, 0.4, 0.5\}$;
- $p \in \{2, 3, 4\}$;
- $n \in \{5, 15\}$;
- $\tau \in \{0.5, 0.75, 0.9, 1.1, 1.25, 1.5\}$;
- $W_U, W_D \in \{0.1, 0.3, 0.6, 0.9\}$;
- $h_S \in \{0.1, 0.5\}$.

These parameters are chosen to cover a large scale of possible scenarios. The shifts $\tau < 1$ present the downward cases and the upwards cases presented by $\tau > 1$. With $n = 5$ and $n = 15$, it is enough to demonstrate the performance of the charts with respect to small sample size and large sample size. As well the values of $W_U(W_D)$, we analyse the variation of the performance from the large warning region to the small warning region. In the Tables 1-6, we present the optimal values of $(\lambda^{+*}, K_U^*, h_L^*)$ for the upward chart, $(\lambda^{-*}, K_D^*, h_L^*)$ for the downward chart, and the values of ATS_1 for each scenario. Moreover, in each table, the second column is devoted to indicate the values of the charts without using variable sampling interval, which was proposed in [16], for the sake of comparison.

As observed in these tables, using variable sampling interval technique improves the performance of the control charts in all cases, the values of ATS_1 are smaller notably than the EWMA charts. For example, in the set-up $\gamma_0 = 0.5, \tau = 1.1, n = 5, p = 2$, the ATS_1 of EWMA chart is 74.71, the ATS_1 is improved to 44.77 when VSI is integrated with $h_S = 0.1$ and $W = 0.1$. The implementation of VSI is simple and does not complicate the calculation significantly. With respect to the change of W in these examples, the increase of W is equivalent to the smaller h_L , which shrinks the warning region. As a result, the performance is better when W is small. For instance, in the set-up $\gamma_0 = 0.1, h_S = 0.1, \tau = 0.75, n = 5, p = 2$, the values of ATS_1 with $W = 0.3$ and $W = 0.9$ are 7.65 and 9.48, respectively. Similar to the other control charts using VSI technique, smaller values of $h_S, h_S = 0.1$, the better results are obtained, compared to $h_S = 0.5$.

It is noted that the higher γ_0 increases the average number of samples needed to detect a process shift, especially when with the small shifts. However, when the sample size is increased, the performance of the control charts are greatly improved. The increase of sample size is also important when there are more variables monitored. For example, in the case of $p = 4$ (Tables 5, 6), with

the shift size $\tau = 0.9$, $\gamma_0 = 0.5$, the other parameters are $h_S = 0.1$, $W = 0.1$, the average time to signal ATS_1 is 78.51 with sample size $n = 5$, and 15.83 with the sample size $n = 15$. Therefore, a large sample size is highly recommended when the practitioner require to monitor many variables simultaneously.

PLEASE INSERT TABLES 1-6 HERE

Finally, the comparisons with the other former methods such as Synthetic MCV [29], Adaptive MCV [22], and Run Sum MCV [23] are executed. Table 7 presents the comparison of VSI EWMA MCV control chart with the adaptive MCV and synthetic MCV control charts. Only the upward control charts are investigated and the parameters used in [22] are $\gamma_0 = \{0.1, 0.3, 0.5\}$, $p = \{2, 3\}$, $\tau = \{1.25, 1.5\}$ and $n = 5$. We can see that the VSI EWMA outperforms both VSSI and synthetic designs in most cases. Only one case with $p = 2$, $\gamma_0 = 0.1$ with large shift $\tau = 1.5$, the VSSI method obtains a slightly better result than VSI EWMA, i.e. $ATS_1 = 4.19$ compared to $ATS_1 = 4.33$. In Table , we show the comparison with the Run Sum MCV, and our proposed design, VSI EWMA, outperform the Run Sum method in every scenario.

PLEASE INSERT TABLES 7-8 HERE

6 Linear covariate error model for the multivariate coefficient of variation

We briefly present, in this section, the linear covariate error model for the sample MCV, which has been considered in [6,4]. Considering a set of independent samples $\{\mathbf{X}_{i1}, \mathbf{X}_{i2}, \dots, \mathbf{X}_{in}\}$ selected at time i -th, $i = 1, 2, \dots$, and \mathbf{X}_{ij} , $j = 1, 2, \dots, n$, is a p -variate random vector following a multivariate normal distribution with the mean vector $\boldsymbol{\mu}$ and the covariance matrix $\boldsymbol{\Sigma}$, where both are known. Due to the measurement error, the true value of \mathbf{X}_{ij} cannot be observed directly. Instead, we can only assess this value via m observations $\{\mathbf{X}_{ij1}^*, \mathbf{X}_{ij2}^*, \dots, \mathbf{X}_{ijm}^*\}$, $m \geq 1$. The relationship between the true value and measured value is suggested by the following linear covariate error model:

$$\mathbf{X}_{ijk}^* = \mathbf{A} + \mathbf{B}\mathbf{X}_{ij} + \boldsymbol{\varepsilon}_{ijk}, \quad k = 1, 2, \dots, m, \quad (14)$$

where \mathbf{A} a p -variate constant vector, \mathbf{B} is a $p \times p$ diagonal constant matrix, and $\boldsymbol{\varepsilon}_{ijk}$ is a random vector of errors following a multivariate normal distribution with the null mean vector and the covariance matrix $\boldsymbol{\Sigma}_{\boldsymbol{\varepsilon}}$, $\boldsymbol{\varepsilon}_{ijk}$ is independent of \mathbf{X}_{ij} . As described in [6], from (14), the following relation is derived

$$\mathbf{Z}_{ijk}^* = \mathbf{B}^{-1}(\mathbf{X}_{ijk}^* - \mathbf{A}) = \mathbf{X}_{ij} + \mathbf{B}^{-1}\boldsymbol{\varepsilon}_{ijk}. \quad (15)$$

Then, \mathbf{Z}_{ijk}^* follows a multivariate normal distribution with the mean vector $\boldsymbol{\mu}$ and the covariance matrix $\boldsymbol{\Sigma} + (\mathbf{B}^{-1})^T \boldsymbol{\Sigma}_{\boldsymbol{\varepsilon}} \mathbf{B}^{-1}$. Consequently, the sample mean vector $\bar{\mathbf{Z}}_{ij}^*$ follows a multivariate normal distribution with the mean

vector $\boldsymbol{\mu}$ and the covariance matrix $\boldsymbol{\Sigma} + \frac{1}{m}(\mathbf{B}^{-1})^T \boldsymbol{\Sigma}_\epsilon \mathbf{B}^{-1}$, the detail can be found in [6]. The population MCV with measurement error (γ^*) based on the quantity $\bar{\mathbf{Z}}_{ij}^*$ is then given by

$$\gamma^* = \left(\boldsymbol{\mu}^T \boldsymbol{\Sigma}^{-1} \left(\mathbf{I} + \frac{1}{m}(\mathbf{B}^{-1})^T \boldsymbol{\Sigma}_\epsilon \mathbf{B}^{-1} \right)^{-1} \boldsymbol{\mu} \right)^{-\frac{1}{2}}. \quad (16)$$

Ayyoub et al. [6] also showed that the population MCV with measurement error can be written as:

$$\gamma^* = \gamma \left(\frac{mB^2}{mB^2 + \theta^2} \right)^{-\frac{1}{2}}, \quad (17)$$

where θ^2 is the measurement error ratio, B is the diagonal element in matrix \mathbf{B} , and γ is defined as (1).

Let $\bar{\bar{\mathbf{Z}}}_i^*$ and \mathbf{S}_i^* be the sample mean and the sample covariance matrix of $\bar{\mathbf{Z}}_{i1}^*, \bar{\mathbf{Z}}_{i2}^*, \dots, \bar{\mathbf{Z}}_{in}^*$, i.e.,

$$\bar{\bar{\mathbf{Z}}}_i^* = \frac{1}{n} \sum_{j=1}^n \bar{\mathbf{Z}}_{ij}^*,$$

and

$$\mathbf{S}_i^* = \frac{1}{n-1} \sum_{j=1}^n (\bar{\mathbf{Z}}_{ij}^* - \bar{\bar{\mathbf{Z}}}_i^*)(\bar{\mathbf{Z}}_{ij}^* - \bar{\bar{\mathbf{Z}}}_i^*)^T.$$

Then, the sample multivariate coefficient of variation $\hat{\gamma}_i^*$ is defined as

$$\hat{\gamma}_i^* = \left(\bar{\bar{\mathbf{Z}}}_i^{*T} \mathbf{S}_i^{*-1} \bar{\bar{\mathbf{Z}}}_i^* \right)^{-\frac{1}{2}}. \quad (18)$$

By replacing γ with γ^* in (3), the cdf of $\hat{\gamma}^{*2}$ is obtained as follows

$$F_{\hat{\gamma}^{*2}}(x | n, p, \gamma^*) = 1 - F_F \left(\frac{n(n-p)}{(n-1)px} \mid p, n-p, \frac{n}{\gamma^{*2}} \right), \quad (19)$$

where $F_F(\cdot | p, n-p, n/\gamma^{*2})$ is the non-central F distribution with p and $n-p$ degrees of freedom and non-centrality parameter n/γ^{*2} .

7 Effect of the measurement error on one-sided VSI EWMA MCV control charts

We investigate, in this Section, the statistical performance of the one-sided VSI EWMA- γ^2 control charts in the present of the measurement errors. Using the linear covariate error model, we can calculate the ATS_1 values with the specific values of n, p, B, m, γ_0 , and θ^2 for the downward and upward VSI EWMA- γ^2 control charts. For the EWMA model, we assume the value $\lambda = 0.2$, which is

a good compromise solution for the EWMA chart to detect effectively small process shifts [28].

Figures 3, 4, 5, 6, 7, and 8 illustrate the effect of the measurement error on the performance of both downward and downward VSI EWMA- γ^2 charts under a single measurement per sample, i.e., $m = 1$. In particular, we plot the ATS_1 curves with respect to the shift size, $\tau \in [0.75, 0.95]$ for downward cases, $\tau \in [1.05, 1.25]$ for upward cases, with $p = 2, n = 5$ and various values of measurement error. The VSI parameters in these illustrations are $h_S \in \{0.1, 0.5\}$ and $W \in \{0.3, 0.9\}$. Specifically, we plot in Figures 3, 4, and 5 the ATS_1 curves for a fixed $B = 1$ and some measurement error ratio $\theta^2 \in \{0, 0.3, 0.5, 1\}$; Figures 6, 7, and 8 display the ATS_1 curves for a fixed $\theta^2 = 0.3$ and several values of the linearity error $B \in \{1, 5\}$. There are few noteworthy observations obtained from these results:

- As observed in Figures 3, 4, 5, the ATS curves corresponding to larger values of θ^2 are above the ones corresponding to the smaller values of θ^2 . That is to say the ATS will get larger when we have more measurement error ratio θ^2 . Moreover, the gap becomes larger when the shift size τ gets smaller.
- On the effect of the linearity error B , from the Figures 6, 7, and 8, the ATS curves corresponding to smaller B are above the ones corresponding to the larger B . And the gap is also larger with the smaller shift size τ .
- From these Figures, we observe that the effect of the measurement error on the ATS is more significant on the upward charts than the downward charts. In addition, the gaps between the ATS curves are larger and clearer with the bigger values of γ_0 . **The other illustrative examples are presented in Appendix A**

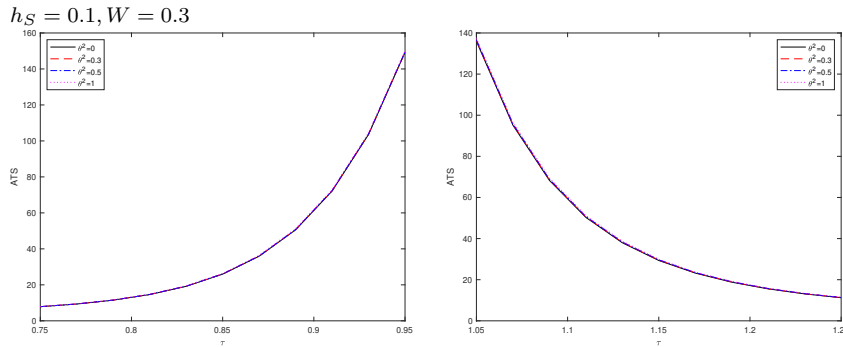


Fig. 3: ATS curves of the downward (left) and upward (right) VSI EWMA MCV charts for $p = 2, \gamma_0 = 0.1, n = 5$ with measurement parameters $B = 1, m = 1$, and $\theta^2 \in \{0, 0.3, 0.5, 1\}$.

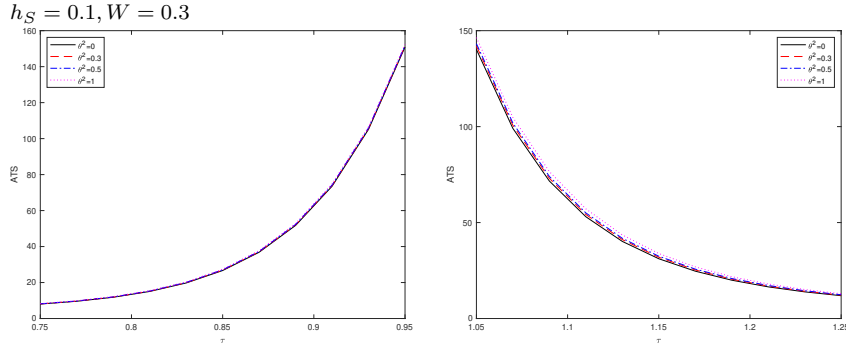


Fig. 4: ATS curves of the downward (left) and upward (right) VSI EWMA MCV charts for $p = 2, \gamma_0 = 0.2, n = 5$ with measurement parameters $B = 1, m = 1$, and $\theta^2 \in \{0, 0.3, 0.5, 1\}$.

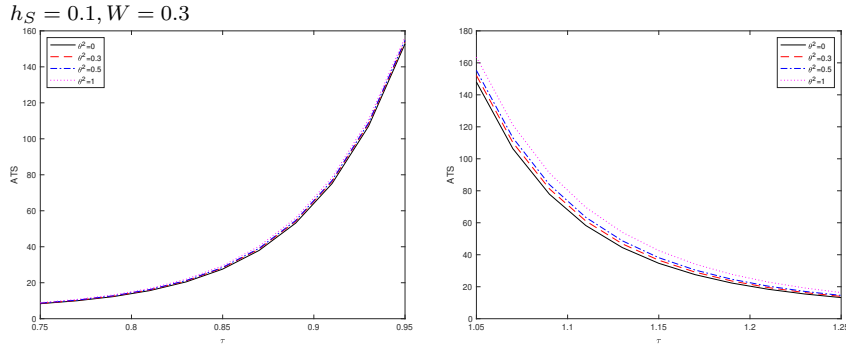


Fig. 5: ATS curves of the downward (left) and upward (right) VSI EWMA MCV charts for $p = 2, \gamma_0 = 0.3, n = 5$ with measurement parameters $B = 1, m = 1$, and $\theta^2 \in \{0, 0.3, 0.5, 1\}$.

8 Illustrative example

In this Section, an illustrative example is presented, in order to help practitioners to apply the upward VSI EWMA chart for the MCV. The data and the context are taken from [16]. In this example, the rate of return of some investments in $p = 3$ different industrial sectors (namely, $S_1 = \text{automotive}$, $S_2 = \text{aeronautic}$ and $S_3 = \text{electronic}$) and in $n = 5$ geographical regions ($R_1 = \text{Africa}$, $R_2 = \text{North America}$, $R_3 = \text{South America}$, $R_4 = \text{Asia}$ and $R_5 = \text{Europe}$) is considered. So, for each instant of time being considered, for each sector S_j and each region R_i , the observed value $X_{i,j}$ represents the rate of return of the investment in sector S_j in region R_i at that moment. The MCV of the rate of return is regarded as a measure of the relative volatility or risk

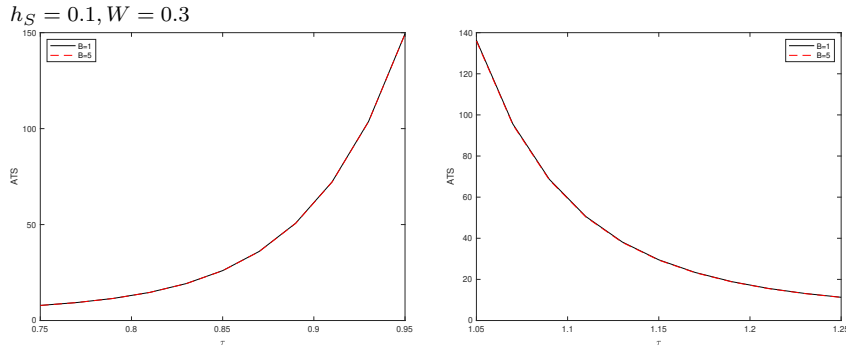


Fig. 6: ATS curves of the downward (left) and upward (right) VSI EWMA MCV charts for $p = 2, \gamma_0 = 0.1, n = 5$ with measurement parameters $\theta^2 = 0.3, m = 1$, and $B \in \{1, 5\}$.

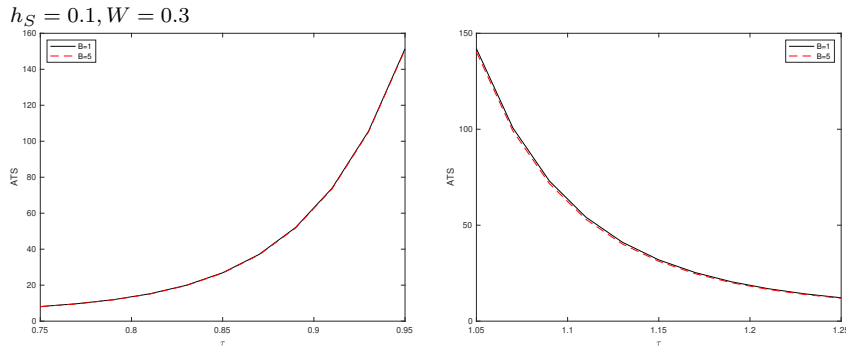


Fig. 7: ATS curves of the downward (left) and upward (right) VSI EWMA MCV charts for $p = 2, \gamma_0 = 0.2, n = 5$ with measurement parameters $\theta^2 = 0.3, m = 1$, and $B \in \{1, 5\}$.

of the investment, and this is why it makes sense to monitor it over time. **More precisely, by measuring the MCV of the rate of return of the three investments at different moments in time, and monitoring it through a properly tuned control chart, we are able to detect when the risk of our investments is increasing in an undesired way. See more details about the justification of this example in [16].**

Let us consider the following input information, which should be obtained from previous knowledge of the process:

- $p = 3$, the number of quality characteristics composing the process.
- $n = 5$, the sample size.
- $\gamma_0 = 0.0404684$, the target value of the MCV (or an estimation of it).

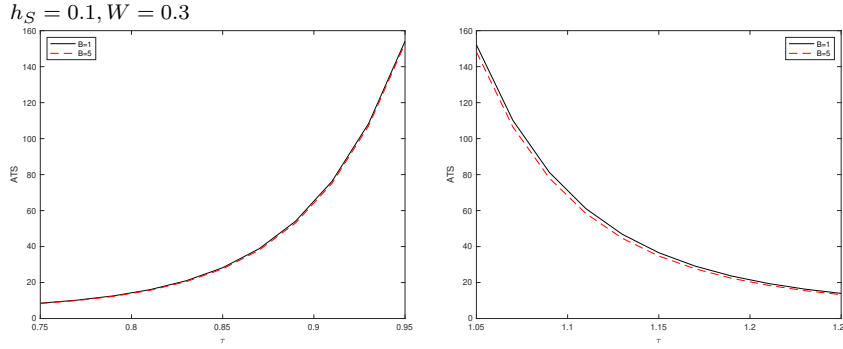


Fig. 8: ATS curves of the downward (left) and upward (right) VSI EWMA MCV charts for $p = 2, \gamma_0 = 0.3, n = 5$ with measurement parameters $\theta^2 = 0.3, m = 1$, and $B \in \{1, 5\}$.

- $h_S = 0.5$ **years**, the shortest possible time between two consecutive sampling operations.
- $\tau = 2$, the (undesirable) shift to detect in the MCV, defined as in (6).
- $W_U = 0.9$, the warning limit coefficient (see Sections 3 and 4 for more details).
- $ATS_0 = 370.4$ **years**.

From this input information, the following can be computed [16]:

- $\mu_0(\hat{\gamma}^2) = 0.000819114$, the expected value of the sample MCV squared when the process is in control or on target.
- $\sigma_0(\hat{\gamma}^2) = 0.000820298$, the standard deviation of the sample MCV squared when the process is in control or on target. The in-control value of ATS is set to include $ATS_0 = 370.4$.

Using this information, we can calculate the optimal values for the parameters of our VSI EWMA chart for the MCV, according to the procedure described in Section 4, the result being:

- $\lambda^{+*} = 0.2886$.
- $K_U^* = 4.0808$.
- $h_L^* = 1.1352$.

From these values for the chart parameters, the limits for the control chart (see Section 3) are easily computable:

- $UCL = 0.002193755$, according to (4).
- $UWL = 0.001122284$, according to (6).

Besides, the average time to detect the undesired shift of $\tau = 2$ in the MCV of this process happens to be $ATS_1 = 2.135$ **years**. The illustration of the upward chart for monitoring $\hat{\gamma}^2$ is shown in Figure 9.

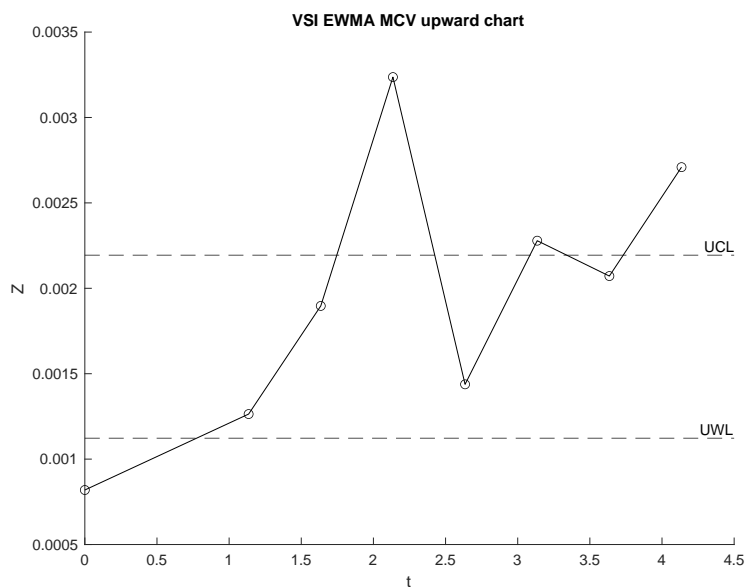


Fig. 9: The upward control chart with $h_S = 0.5$.

9 Concluding remarks

In this paper, two new one-sided control charts for the MCV (aimed at detecting increase and decrease in dispersion, respectively) have been proposed, basing on applying a VSI scheme on an EWMA strategy. Formulas to determine the optimal values of the parameters governing the performance of the charts were derived by using Markov chains. The performance of the chart was compared against several competing charts. The proposed VSI EWMA chart was found to outperform the run-sum chart in [23], the variable sample size and sampling interval (VSSI) chart in [22] and the synthetic chart in [29] in most cases. Consequently, the method can be regarded as an advisable way to monitor the MCV of a normally distributed multivariate process. Furthermore, the evaluation of the effect of measurement errors in the performance of the chart, in the line of [3], has been conducted in this study. From this study, the measurement error was found to have a significant effect on the performance of the charts when the shift size is small and/or the value of γ_0 is large. When γ_0 is small, the role of the measurement error is negligible, especially in the downward charts.

We have provided the details of all the necessary steps and appropriate look-up tables to help practitioners to implement this new control chart. The benefits of applying our approach when monitoring the relative dispersion of a multivariate process are the result of combining the known advantages of the EWMA and the VSI schemes being used (which have been already mentioned

in the introduction of this paper): a higher ability to detect small shifts in the dispersion, and a higher efficiency regarding sampling times and sampling cost.

Further research steps include studying the sensitivity of this chart (and other MCV charts) to lack of normality in the process variables and, consequently, exploring non-parametric alternatives for measuring and efficiently monitoring the relative dispersion of a multivariate process.

Funding

VGB's research work was supported by the Ministerio de Ciencia e Innovación of Spain under grant no. PID2019-110442GB-I00.

Declarations

- The authors have no relevant financial or non-financial interests to disclose.
- The authors have no conflicts of interest to declare that are relevant to the content of this article.
- All authors certify that they have no affiliations with or involvement in any organization or entity with any financial interest or non-financial interest in the subject matter or materials discussed in this manuscript.
- The authors have no financial or proprietary interests in any material discussed in this article.

References

1. Abbasi, S.A., Adegoke, N.A.: Multivariate coefficient of variation control charts in phase I of SPC. *The International Journal of Advanced Manufacturing Technology* **99**(5-8), 1903–1916 (2018)
2. Allison, P.D.: Measures of Inequality. *American Sociological Review* **43**(6), 865–880 (1978)
3. Ayyoub, H.N., Khoo, M.B., Saha, S., Castagliola, P.: Multivariate coefficient of variation charts with measurement errors. *Computers and Industrial Engineering* **147**, Article 106633 (2020)
4. Ayyoub, H.N., Khoo, M.B., Saha, S., Castagliola, P.: Multivariate coefficient of variation charts with measurement errors. *Computers & Industrial Engineering* **147**, 106633 (2020). DOI <https://doi.org/10.1016/j.cie.2020.106633>
5. Ayyoub, H.N., Khoo, M.B., Saha, S., Lee, M.H.: Variable sampling interval ewma chart for multivariate coefficient of variation. *Communications in Statistics-Theory and Methods* pp. 1–21 (2020)
6. Ayyoub, H.N., Khoo, M.B.C., Lee, M.H., Haq, A.: Monitoring multivariate coefficient of variation with upward shewhart and ewma charts in the presence of measurement errors using the linear covariate error model. *Quality and Reliability Engineering International* **37**(2), 694–716 (2021). DOI <https://doi.org/10.1002/qre.2757>.
7. Brook, D., Evans, D.A.: An Approach to the Probability Distribution of Cusum Run Length. *Biometrika* **59**(3), 539–549 (1972)
8. Castagliola, P., Achouri, A., Taleb, H., Celano, G., Psarakis, S.: Monitoring the coefficient of variation using a variable sampling interval control chart. *Quality and Reliability Engineering International* **29**(8), 1135–1149 (2013)

9. Castagliola, P., Achouri, A., Taleb, H., Celano, G., Psarakis, S.: Monitoring the coefficient of variation using a variable sample size control chart. *International Journal of Advanced Manufacturing Technology* **81**(9-12), 1561–1576 (2015)
10. Chew, X., Khaw, K.W.: One-sided Downward Control Chart for Monitoring the Multivariate Coefficient of Variation with VSSI Strategy. *Journal of Mathematical and Fundamental Sciences* **52**(1), 112–130 (2020)
11. Chew, X., Khaw, K.W., Lee, M.H.: The efficiency of run rules schemes for the multivariate coefficient of variation in short runs process. *Communications in Statistics-Simulation and Computation* pp. 1–21 (2020)
12. Chew, X., Khaw, K.W., Yeong, W.C.: The efficiency of run rules schemes for the multivariate coefficient of variation: a markov chain approach. *Journal of Applied Statistics* **47**(3), 460–480 (2020)
13. Chew, X., Khaw, K.W., Yeong, W.C.: The efficiency of run rules schemes for the multivariate coefficient of variation: a Markov chain approach. *Journal of Applied Statistics* **47**(3), 460–480 (2020)
14. Chew, X., Khoo, M.B.C., Khaw, K.W., Yeong, W.C., Chong, Z.L.: A proposed variable parameter control chart for monitoring the multivariate coefficient of variation. *Quality and Reliability Engineering International* **35**(7), 2442–2461 (2019)
15. Cui, R.Q., Reynolds Jr., M.R.: \bar{X} -Chart with runs and variable sampling intervals. *Communications in Statistics - Simulation and Computation* **17**(3), 1073–1093 (1988)
16. Giner-Bosch, V., Tran, K.P., Castagliola, P., Khoo, M.B.C.: An EWMA control chart for the multivariate coefficient of variation. *Quality and Reliability Engineering International* **35**(6), 1515–1541 (2019)
17. Haq, A., Bibi, N., Chong Khoo, M.B.: Enhanced EWMA charts for monitoring the process coefficient of variation. *Quality and Reliability Engineering International* **n/a**(Early view) (2020)
18. Haq, A., Khoo, M.B.: New adaptive EWMA control charts for monitoring univariate and multivariate coefficient of variation. *Computers and Industrial Engineering* **131**, 28–40 (2019)
19. Kang, C., Lee, M., Seon, Y., Hawkins, D.M.: A control chart for the coefficient of variation. *Journal of Quality Technology* **39**(2), 151–158 (2007)
20. Khatun, M., Khoo, M.B., Lee, M.H., Castagliola, P.: One-sided control charts for monitoring the multivariate coefficient of variation in short production runs. *Transactions of the Institute of Measurement and Control* **41**(6), 1712–1728 (2019)
21. Khaw, K.W., Chew, X., Yeong, W.C., Lim, S.L.: Optimal design of the synthetic control chart for monitoring the multivariate coefficient of variation. *Chemometrics and Intelligent Laboratory Systems* **186**, 33–40 (2019)
22. Khaw, K.W., Khoo, M.B., Castagliola, P., Rahim, M.: New adaptive control charts for monitoring the multivariate coefficient of variation. *Computers and Industrial Engineering* **126**, 595–610 (2018)
23. Lim, A.J.X., Khoo, M.B.C., Teoh, W.L., Haq, A.: Run sum chart for monitoring multivariate coefficient of variation. *Computers and Industrial Engineering* **109**, 84–95 (2017)
24. Lucas, J.M., Saccucci, M.S.: Exponentially weighted moving average control schemes: properties and enhancements. *Technometrics* **32**(1), 1–12 (1990)
25. Marquardt, D.W.: An algorithm for least-squares estimation of nonlinear parameters. *Journal of the society for Industrial and Applied Mathematics* **11**(2), 431–441 (1963)
26. Montgomery, D.C.: *Introduction to Statistical Quality Control*, 7 edn. John Wiley & Sons, Hoboken, NJ (2012)
27. Ng, W.C., Khoo, M.B.C., Chong, Z.L., Lee, M.H.: Economic and Economic-Statistical Designs of Multivariate Coefficient of Variation Chart. *REVSTAT - Statistical Journal (Forthcoming papers)* (2019)
28. Nguyen, H.D., Tran, K.P., Celano, G., Maravelakis, P.E., Castagliola, P.: On the effect of the measurement error on shewhart t and ewma t control charts. *The International Journal of Advanced Manufacturing Technology* **107**(9), 4317–4332 (2020)
29. Nguyen, Q.T., Tran, K.P., Castagliola, P., Celano, G., Lardjane, S.: One-sided synthetic control charts for monitoring the multivariate coefficient of variation. *Journal of Statistical Computation and Simulation* **89**(10), 1841–1862 (2019)

30. Nguyen, Q.T., Tran, K.P., Heuchenne, H.L., Nguyen, T.H., Nguyen, H.D.: Variable sampling interval Shewhart control charts for monitoring the multivariate coefficient of variation. *Applied Stochastic Models in Business and Industry* **35**(5), 1253–1268 (2019)
31. Reynolds Jr., M.R., Amin, R.W., Arnold, J.C.: CUSUM Charts With Variable Sampling Intervals. *Technometrics* **32**(4), 371–384 (1990)
32. Reynolds Jr., M.R., Amin, R.W., Arnold, J.C., Nachlas, J.A.: \bar{X} charts with variable sampling intervals. *Technometrics* **30**(2), 181–192 (1988)
33. Ridge, E., Kudenko, D.: Tuning an algorithm using design of experiments. In: T. Bartz-Beielstein, M. Chiarandini, L. Paquete, M. Preuss (eds.) *Experimental Methods for the Analysis of Optimization Algorithms*, chap. 11, pp. 265–286. Springer, New York (2010)
34. Roberts, S.W.: Control Chart Tests Based on Geometric Moving Averages. *Technometrics* **1**(3), 239–250 (1959)
35. Runger, G.C., Montgomery, D.C.: Adaptive sampling enhancements for Shewhart control charts. *IIE Transactions* **25**(3), 41–51 (1993)
36. Runger, G.C., Pignatiello, J.J.: Adaptive Sampling for Process Control. *Journal of Quality Technology* **23**(2), 135–155 (1991)
37. Saccucci, M.S., Amin, R.W., Lucas, J.M.: Exponentially weighted moving average control schemes with variable sampling intervals. *Communications in Statistics - Simulation and Computation* **21**(3), 627–657 (1992)
38. Suárez-Cabello, M.J.: Gráficos de control para el coeficiente de variación multivariante: estado actual y análisis comparativo. Master's Thesis, Universitat Politècnica de València (2019). URL <http://hdl.handle.net/10251/129499>
39. Tagaras, G.: A Survey of Recent Developments in the Design of Adaptive Control Charts. *Journal of Quality Technology* **30**(3), 212–231 (1998)
40. Teoh, W.L., Khoo, M.B.C., Castagliola, P., Yeong, W.C., Teh, S.Y.: Run-sum control charts for monitoring the coefficient of variation. *European Journal of Operational Research* **257**(1), 144–158 (2017)
41. Tran, P.H., Tran, K.P.: The efficiency of CUSUM schemes for monitoring the coefficient of variation. *Applied Stochastic Models in Business and Industry* **32**(6), 870–881 (2016)
42. Tran, P.H., Tran, K.P., Huong, T.T., Heuchenne, C., Nguyen, T.A.D., Do, C.N.: A variable sampling interval ewma distribution-free control chart for monitoring services quality. In: *Proceedings of the 2018 International Conference on E-Business and Applications*, pp. 1–5 (2018)
43. Voinov, V., Nikulin, M.: *Unbiased Estimators and their Applications: Volume 2: Multivariate Case*, vol. 362. Springer Science & Business Media (1996)
44. Yeong, W., Khoo, M.B., Tham, L., Teoh, W., Rahim, M.: Monitoring the coefficient of variation using a variable sampling interval ewma chart. *Journal of Quality Technology* **49**(4), 380–401 (2017)
45. Yeong, W.C., Khoo, M.B.C., Teoh, W.L., Castagliola, P.: A Control Chart for the Multivariate Coefficient of Variation. *Quality and Reliability Engineering International* **32**(3), 1213–1225 (2016)

A Appendix

PLEASE INSERT FIGURES 10-15 HERE

τ	FSI	$h_S = 0.1$				$h_S = 0.5$			
		$\gamma_0 = 0.1$	$W = 0.3$	$W = 0.6$	$W = 0.9$	$W = 0.1$	$W = 0.3$	$W = 0.6$	$W = 0.9$
0.50	(0.2730, 1.7592, 8.31)	(0.4371, 1.5388, 2.570, 3.47)	(0.4227, 1.5526, 1.709, 3.34)	(0.3591, 1.6364, 1.280, 3.98)	(0.3290, 1.6776, 2.259, 6.03)	(0.3188, 1.6923, 1.850, 5.71)	(0.3447, 1.6591, 1.398, 5.46)	(0.3125, 1.7013, 1.163, 5.93)	
0.75	(0.0730, 2.0272, 25.14)	(0.4933, 1.4666, 2.882, 3.90)	(0.4721, 1.5388, 2.570, 3.47)	(0.4025, 1.5974, 1.812, 4.30)	(0.3683, 1.6561, 1.383, 4.59)	(0.3391, 1.7076, 1.958, 5.86)	(0.3572, 1.6845, 1.468, 5.79)	(0.3439, 1.6643, 1.160, 6.01)	
0.90	(0.0171, 1.8902, 77.21)	(0.0258, 1.9255, 6.038, 42.00)	(0.0225, 1.9263, 2.961, 44.47)	(0.0211, 1.9133, 1.740, 40.34)	(0.0198, 1.9098, 3.861, 57.81)	(0.0200, 1.9008, 2.697, 59.10)	(0.0211, 1.9131, 1.416, 61.80)	(0.0219, 1.9224, 1.180, 65.32)	
1.10	(0.0150, 2.0620, 79.22)	(0.0196, 2.2137, 5.608, 45.25)	(0.0219, 2.2700, 2.909, 46.67)	(0.0180, 2.1647, 1.565, 50.46)	(0.0175, 2.1495, 2.472, 57.29)	(0.0169, 2.1301, 1.722, 58.02)	(0.0180, 2.1650, 1.314, 60.24)	(0.0200, 2.2251, 1.152, 63.03)	
1.25	(0.0482, 2.7478, 241.8)	(0.0759, 3.0415, 2.704, 13.54)	(0.0643, 2.9312, 2.102, 13.50)	(0.0532, 2.8089, 1.580, 14.18)	(0.0624, 2.9114, 2.030, 18.37)	(0.0585, 2.8700, 1.635, 18.63)	(0.0531, 2.8987, 1.322, 18.63)	(0.0515, 2.7892, 1.172, 19.29)	
1.50	(0.1157, 3.3410, 9.35)	(0.2157, 3.8444, 2.102, 5.71)	(0.1792, 3.6884, 1.791, 5.54)	(0.1550, 3.5676, 1.484, 5.56)	(0.1680, 3.6331, 1.700, 7.51)	(0.1492, 3.5369, 1.482, 7.37)	(0.1300, 3.4291, 1.276, 7.35)	(0.1181, 3.3562, 1.165, 7.47)	
0.50	(0.2733, 1.7255, 8.42)	(0.4918, 1.4366, 2.927, 3.97)	(0.4113, 1.5388, 2.418, 3.52)	(0.4251, 1.5173, 1.700, 3.40)	(0.3272, 1.6469, 2.291, 6.12)	(0.3051, 1.6784, 1.877, 5.78)	(0.3478, 1.6185, 1.391, 5.76)	(0.3149, 1.6643, 1.160, 6.01)	
0.75	(0.0730, 2.0272, 25.14)	(0.1192, 1.9710, 4.448, 10.77)	(0.1141, 1.9786, 2.915, 10.76)	(0.1041, 1.9930, 1.802, 13.04)	(0.0994, 2.0106, 3.204, 17.38)	(0.0902, 2.0109, 2.152, 17.28)	(0.0876, 2.0141, 1.441, 17.90)	(0.0841, 2.0178, 1.199, 18.81)	
0.90	(0.0171, 1.8902, 78.50)	(0.0237, 1.9260, 6.131, 43.03)	(0.0226, 1.8884, 1.724, 30.66)	(0.0202, 1.8884, 1.724, 30.66)	(0.0207, 1.8941, 3.015, 58.90)	(0.0202, 1.8877, 2.112, 60.21)	(0.0224, 1.9132, 1.421, 63.01)	(0.0201, 1.8863, 1.178, 66.57)	
1.10	(0.0150, 2.0620, 79.22)	(0.0171, 2.2677, 5.640, 45.28)	(0.0165, 2.2571, 2.102, 45.27)	(0.0154, 2.2692, 1.580, 49.50)	(0.0158, 2.2809, 2.032, 59.02)	(0.0151, 2.2632, 1.603, 58.96)	(0.0154, 2.2808, 1.316, 63.32)	(0.0149, 2.2809, 1.169, 66.01)	
1.25	(0.0484, 2.7131, 251.63)	(0.0717, 3.0255, 2.704, 14.00)	(0.0598, 2.9200, 2.104, 13.90)	(0.0514, 2.8087, 1.580, 15.08)	(0.0582, 2.8889, 2.032, 19.02)	(0.0524, 2.8216, 1.693, 18.96)	(0.0514, 2.8088, 1.316, 19.32)	(0.0499, 2.7890, 1.169, 20.01)	
1.50	(0.1043, 3.3066, 10.00)	(0.2025, 3.8628, 2.114, 5.93)	(0.1676, 3.6941, 1.791, 5.77)	(0.1448, 3.5678, 1.480, 5.81)	(0.1544, 3.6231, 1.714, 7.85)	(0.1289, 3.4735, 1.468, 7.69)	(0.1197, 3.4132, 1.276, 7.69)	(0.1112, 3.3560, 1.162, 7.83)	
0.50	(0.2733, 1.7255, 8.42)	(0.4917, 1.3896, 3.000, 4.07)	(0.4195, 1.4666, 2.430, 3.58)	(0.4257, 1.4506, 1.677, 3.52)	(0.3275, 1.5671, 2.341, 6.27)	(0.3114, 1.6097, 1.881, 5.91)	(0.3522, 1.5533, 1.391, 5.91)	(0.3114, 1.6098, 1.151, 6.17)	
0.75	(0.0731, 1.9791, 25.89)	(0.1179, 1.9179, 4.599, 11.18)	(0.1139, 1.9242, 3.018, 11.16)	(0.1046, 1.9389, 1.792, 12.40)	(0.0988, 1.9608, 3.179, 17.89)	(0.0909, 1.9587, 2.115, 17.88)	(0.0876, 1.9629, 1.434, 18.51)	(0.0830, 1.9684, 1.196, 19.45)	
0.90	(0.0171, 1.8290, 80.72)	(0.0237, 1.8962, 6.301, 44.70)	(0.0226, 1.8862, 1.739, 52.44)	(0.0205, 1.8857, 1.739, 52.44)	(0.0206, 1.8965, 4.004, 60.81)	(0.0202, 1.8915, 2.091, 62.29)	(0.0200, 1.8993, 1.411, 65.04)	(0.0193, 1.8907, 1.172, 68.76)	
1.10	(0.0150, 2.0620, 79.22)	(0.0170, 2.1444, 3.503, 48.67)	(0.0166, 2.1291, 2.225, 50.37)	(0.0157, 2.0953, 1.524, 54.88)	(0.0148, 2.1032, 2.442, 61.31)	(0.0134, 2.1003, 1.675, 62.27)	(0.0127, 1.9714, 1.278, 64.88)	(0.0124, 2.0853, 1.134, 67.82)	
1.25	(0.0382, 2.6431, 264.0)	(0.0650, 3.0091, 2.703, 14.81)	(0.0531, 2.8993, 2.104, 14.88)	(0.0452, 2.7890, 1.292, 17.14)	(0.0516, 2.8446, 2.042, 20.21)	(0.0463, 2.7731, 1.399, 20.17)	(0.0415, 2.6970, 1.307, 20.62)	(0.0328, 2.7128, 1.162, 21.38)	
1.50	(0.0876, 3.2369, 10.83)	(0.1863, 3.8722, 2.135, 6.32)	(0.1465, 3.6963, 1.790, 6.17)	(0.1302, 3.5676, 1.471, 6.29)	(0.1341, 3.5944, 1.755, 8.47)	(0.1192, 3.5002, 1.491, 8.32)	(0.1053, 3.3848, 1.274, 8.33)	(0.0929, 3.2824, 1.153, 8.51)	
0.50	(0.2733, 1.5089, 8.83)	(0.4895, 1.2941, 3.069, 4.20)	(0.4041, 1.3929, 2.481, 3.69)	(0.4308, 1.3609, 1.629, 3.72)	(0.3262, 1.4929, 2.421, 6.50)	(0.3029, 1.5252, 1.906, 6.09)	(0.3508, 1.4506, 1.361, 6.18)	(0.3128, 1.5115, 1.131, 6.44)	
0.75	(0.0732, 1.8985, 26.98)	(0.1170, 1.8259, 4.830, 11.80)	(0.1155, 1.8286, 3.006, 11.82)	(0.0971, 1.8592, 1.790, 13.13)	(0.0894, 1.8716, 3.312, 18.73)	(0.0828, 1.8662, 2.095, 18.76)	(0.0874, 1.8746, 1.434, 19.39)	(0.0795, 1.8857, 1.187, 20.45)	
0.90	(0.0181, 1.7831, 83.99)	(0.0238, 1.8401, 6.573, 47.23)	(0.0233, 1.8364, 2.978, 49.98)	(0.0203, 1.8087, 1.734, 55.38)	(0.0211, 1.8168, 4.147, 63.65)	(0.0206, 1.8120, 2.101, 65.16)	(0.0203, 1.8084, 1.408, 68.12)	(0.0211, 1.8169, 1.170, 72.02)	
1.10	(0.0099, 1.8184, 81.89)	(0.0147, 2.0477, 3.437, 52.14)	(0.0119, 1.9243, 2.095, 54.59)	(0.0159, 2.0954, 1.488, 59.52)	(0.0146, 2.0434, 1.219, 65.41)	(0.0135, 2.0002, 1.628, 66.74)	(0.0129, 1.8795, 1.260, 69.62)	(0.0136, 2.0016, 1.118, 73.04)	
1.25	(0.0306, 2.5087, 29.20)	(0.0511, 2.8702, 2.025, 16.32)	(0.0401, 2.6941, 1.513, 17.44)	(0.0412, 2.7132, 1.268, 19.11)	(0.0429, 2.7429, 2.048, 22.16)	(0.0387, 2.6694, 1.591, 22.16)	(0.0401, 2.6939, 1.285, 22.74)	(0.0386, 2.5722, 1.147, 23.67)	
1.50	(0.0682, 3.0987, 12.27)	(0.1222, 3.8346, 2.162, 6.95)	(0.1260, 3.6417, 1.787, 6.82)	(0.0994, 3.4172, 1.455, 7.00)	(0.1083, 3.4964, 1.765, 9.49)	(0.0951, 3.3774, 1.467, 9.34)	(0.0959, 3.3846, 1.257, 9.40)	(0.0819, 3.2460, 1.147, 9.61)	
0.50	(0.2730, 1.4039, 9.95)	(0.4188, 1.1575, 3.106, 4.93)	(0.4016, 1.2493, 2.468, 3.89)	(0.3174, 1.3939, 1.514, 4.30)	(0.3254, 1.3346, 2.408, 6.77)	(0.3159, 1.3469, 1.862, 6.32)	(0.3092, 1.3771, 1.319, 6.54)	(0.2876, 1.3847, 1.097, 6.93)	
0.75	(0.0734, 1.7308, 28.48)	(0.1158, 1.6694, 4.989, 12.62)	(0.1154, 1.6793, 1.757, 14.37)	(0.0924, 1.6968, 1.724, 16.00)	(0.0944, 1.7095, 3.515, 19.80)	(0.0857, 1.6969, 2.098, 19.98)	(0.0853, 1.7153, 1.435, 20.68)	(0.0831, 1.7189, 1.150, 23.09)	
0.90	(0.0192, 1.6859, 88.46)	(0.0240, 1.7304, 2.970, 53.87)	(0.0223, 1.7083, 1.673, 60.65)	(0.0200, 1.6926, 1.269, 67.71)	(0.0222, 1.7097, 4.382, 67.65)	(0.0207, 1.7079, 2.095, 69.31)	(0.0229, 1.7133, 1.393, 72.55)	(0.0200, 1.6927, 1.180, 76.94)	
1.10	(0.0098, 1.5420, 89.63)	(0.0110, 1.8070, 3.137, 57.54)	(0.0126, 1.8987, 1.971, 60.87)	(0.0139, 1.9146, 1.896, 67.42)	(0.0090, 1.6954, 2.235, 71.94)	(0.0090, 1.6936, 1.515, 73.83)	(0.0101, 1.7613, 1.204, 77.62)	(0.0112, 1.8175, 1.088, 81.76)	
1.25	(0.0220, 2.2311, 33.31)	(0.0445, 2.7255, 2.675, 18.16)	(0.0363, 2.5790, 1.902, 18.67)	(0.0371, 2.5884, 1.437, 21.42)	(0.0325, 2.4937, 2.045, 25.17)	(0.0303, 2.4452, 1.534, 25.31)	(0.0284, 2.4005, 1.242, 26.18)	(0.0303, 2.4458, 1.120, 27.44)	
1.50	(0.0487, 2.7985, 14.53)	(0.1198, 3.6254, 2.188, 7.89)	(0.0966, 3.4015, 1.730, 7.84)	(0.0800, 3.2198, 1.409, 8.19)	(0.0802, 3.2231, 1.798, 11.09)	(0.0703, 3.1023, 1.438, 10.95)	(0.0678, 3.0794, 1.292, 11.10)	(0.0542, 2.8819, 1.124, 11.48)	

Table 3: The parameters λ^- , K_D , h_L , ATS_1 and λ^+ , K_U , h_L , ATS_1 of the VSI EWMA- γ^2 control charts compared with those λ^- , K_D , ARL_1 and λ^+ , K_U , ARL_1 of FSI EWMA charts (second column) for $p = 3$, $n = 5$, $\gamma_0 = \{0.1, 0.2, 0.3, 0.4, 0.5\}$, $\tau = \{0.5, 0.75, 0.9, 1.1, 1.25, 1.5\}$ and $ATS_0 = 370.4$.

τ	FSI	$h_S=0.1$					$h_S=0.5$				
		$\gamma_0=0.1$	$W=0.3$	$W=0.6$	$W=0.9$	$W=1.5$	$\gamma_0=0.1$	$W=0.3$	$W=0.6$	$W=0.9$	$W=1.5$
0.50	(0.8580, 1.9400, 1.98)	(0.9915, 1.8876, 1.869, 1.81)	(0.9454, 1.9058, 1.897, 1.50)	(0.9051, 1.9233, 1.912, 1.32)	(0.8698, 1.9258, 1.958, 2.06)	(0.8849, 1.9309, 1.407, 1.90)	(0.8714, 1.9303, 1.237, 1.73)	(0.8633, 1.9406, 1.124, 1.62)			
0.75	(0.8621, 2.0015, 6.62)	(0.9958, 1.9698, 2.063, 3.10)	(0.9750, 2.3276, 1.767, 13.05)	(0.9712, 2.2958, 1.821, 3.11)	(0.9370, 2.2573, 1.968, 4.97)	(0.9026, 2.2774, 1.861, 4.60)	(0.8982, 2.2774, 1.861, 4.60)	(0.8873, 1.9041, 1.124, 1.64)			
0.90	(0.8684, 2.2882, 26.15)	(0.9881, 2.3443, 3.888, 11.37)	(0.9846, 2.3369, 2.706, 11.36)	(0.9688, 2.3220, 1.801, 14.78)	(0.9340, 2.2870, 2.436, 15.35)	(0.9076, 2.3189, 2.745, 18.41)	(0.9076, 2.3189, 2.745, 18.41)	(0.8910, 2.3015, 1.201, 19.85)			
1.10	(0.8730, 3.1376, 25.05)	(0.9958, 2.7883, 8.161, 12.80)	(0.9892, 2.7232, 2.315, 12.60)	(0.9709, 2.6930, 1.375, 14.16)	(0.9478, 2.6385, 2.706, 17.85)	(0.9198, 2.6238, 1.963, 17.78)	(0.9198, 2.6238, 1.963, 17.78)	(0.8977, 2.6402, 1.191, 19.46)			
1.25	(0.8773, 3.1876, 6.91)	(0.9915, 3.4337, 2.154, 3.92)	(0.9868, 3.3751, 1.815, 3.71)	(0.9688, 3.2712, 1.518, 3.64)	(0.9478, 3.2884, 1.761, 5.36)	(0.9237, 3.2420, 1.522, 5.18)	(0.9237, 3.2420, 1.522, 5.18)	(0.9014, 3.1718, 1.174, 5.18)			
1.50	(0.8294, 3.5389, 2.61)	(0.8511, 3.7536, 1.608, 2.82)	(0.7532, 3.7415, 1.520, 1.94)	(0.5428, 3.6780, 1.242, 1.74)	(0.6533, 3.7058, 1.437, 2.38)	(0.5892, 3.6706, 1.333, 2.27)	(0.5892, 3.6706, 1.333, 2.27)	(0.4770, 3.5851, 1.136, 2.13)			
0.50	(0.8524, 1.9084, 2.03)	(0.9999, 1.8447, 1.960, 2.09)	(0.9522, 1.8515, 1.687, 1.81)	(0.9083, 1.8657, 1.210, 1.32)	(0.8911, 1.8889, 1.570, 2.09)	(0.8988, 1.8857, 1.401, 1.93)	(0.8651, 1.9005, 1.236, 1.75)	(0.8573, 1.9041, 1.124, 1.64)			
0.75	(0.8621, 2.0015, 6.62)	(0.9999, 2.1471, 2.456, 3.42)	(0.9806, 2.1471, 2.456, 3.42)	(0.9712, 2.2258, 1.821, 3.11)	(0.9370, 2.2573, 1.968, 4.97)	(0.9026, 2.2774, 1.861, 4.60)	(0.9026, 2.2774, 1.861, 4.60)	(0.8910, 2.3015, 1.201, 19.85)			
0.90	(0.8684, 2.2882, 26.15)	(0.9881, 2.3443, 3.888, 11.37)	(0.9846, 2.3369, 2.706, 11.36)	(0.9688, 2.3220, 1.801, 14.78)	(0.9340, 2.2870, 2.436, 15.35)	(0.9076, 2.3189, 2.745, 18.41)	(0.9076, 2.3189, 2.745, 18.41)	(0.8910, 2.3015, 1.201, 19.85)			
1.10	(0.8730, 3.1376, 25.05)	(0.9958, 2.7883, 8.161, 12.80)	(0.9892, 2.7232, 2.315, 12.60)	(0.9709, 2.6930, 1.375, 14.16)	(0.9478, 2.6385, 2.706, 17.85)	(0.9198, 2.6238, 1.963, 17.78)	(0.9198, 2.6238, 1.963, 17.78)	(0.8977, 2.6402, 1.191, 19.46)			
1.25	(0.8773, 3.1876, 6.91)	(0.9915, 3.4337, 2.154, 3.92)	(0.9868, 3.3751, 1.815, 3.71)	(0.9688, 3.2712, 1.518, 3.64)	(0.9478, 3.2884, 1.761, 5.36)	(0.9237, 3.2420, 1.522, 5.18)	(0.9237, 3.2420, 1.522, 5.18)	(0.9014, 3.1718, 1.174, 5.18)			
1.50	(0.8294, 3.5389, 2.61)	(0.8511, 3.7536, 1.608, 2.82)	(0.7532, 3.7415, 1.520, 1.94)	(0.5428, 3.6780, 1.242, 1.74)	(0.6533, 3.7058, 1.437, 2.38)	(0.5892, 3.6706, 1.333, 2.27)	(0.5892, 3.6706, 1.333, 2.27)	(0.4770, 3.5851, 1.136, 2.13)			
0.50	(0.8432, 1.8487, 2.12)	(0.9987, 1.7822, 1.988, 2.13)	(0.9720, 1.7925, 1.717, 1.85)	(0.9333, 1.8683, 1.200, 1.81)	(0.8823, 1.8302, 1.591, 2.16)	(0.8695, 1.8361, 1.422, 1.98)	(0.8565, 1.8428, 1.239, 1.80)	(0.8473, 1.8487, 1.124, 1.68)			
0.75	(0.8568, 2.0015, 6.62)	(0.9987, 2.1024, 2.518, 3.35)	(0.9720, 2.1024, 2.518, 3.35)	(0.9641, 2.1821, 1.632, 3.28)	(0.9319, 2.1337, 2.328, 3.28)	(0.9052, 2.1337, 2.328, 3.28)	(0.8929, 2.1337, 2.328, 3.28)	(0.8843, 1.8487, 1.124, 1.68)			
0.90	(0.8618, 2.2882, 26.15)	(0.9889, 2.3119, 4.009, 12.64)	(0.9811, 2.3045, 2.760, 12.64)	(0.9665, 2.2827, 1.869, 15.60)	(0.9405, 2.2590, 2.808, 19.35)	(0.9180, 2.2590, 2.808, 19.35)	(0.9180, 2.2590, 2.808, 19.35)	(0.9033, 2.2779, 1.206, 20.87)			
1.10	(0.8648, 3.1376, 25.05)	(0.9958, 2.7883, 8.161, 12.80)	(0.9892, 2.7232, 2.315, 12.60)	(0.9709, 2.6930, 1.375, 14.16)	(0.9478, 2.6385, 2.706, 17.85)	(0.9198, 2.6238, 1.963, 17.78)	(0.9198, 2.6238, 1.963, 17.78)	(0.9033, 2.2779, 1.206, 20.87)			
1.25	(0.8684, 3.1876, 6.91)	(0.9915, 3.4337, 2.154, 3.92)	(0.9868, 3.3751, 1.815, 3.71)	(0.9688, 3.2712, 1.518, 3.64)	(0.9478, 3.2884, 1.761, 5.36)	(0.9237, 3.2420, 1.522, 5.18)	(0.9237, 3.2420, 1.522, 5.18)	(0.9033, 2.2779, 1.206, 20.87)			
1.50	(0.8294, 3.5389, 2.61)	(0.8511, 3.7536, 1.608, 2.82)	(0.7532, 3.7415, 1.520, 1.94)	(0.5428, 3.6780, 1.242, 1.74)	(0.6533, 3.7058, 1.437, 2.38)	(0.5892, 3.6706, 1.333, 2.27)	(0.5892, 3.6706, 1.333, 2.27)	(0.4770, 3.5851, 1.136, 2.13)			
0.50	(0.8295, 1.7739, 2.33)	(0.9857, 1.7041, 2.036, 2.19)	(0.9576, 1.7151, 1.737, 1.88)	(0.9255, 1.7922, 1.202, 1.34)	(0.8710, 1.7529, 1.619, 2.24)	(0.8569, 1.7598, 1.434, 2.05)	(0.8505, 1.7600, 1.237, 1.85)	(0.8432, 1.7720, 1.118, 1.74)			
0.75	(0.8505, 2.0015, 6.62)	(0.9857, 2.0421, 2.606, 3.73)	(0.9705, 2.0421, 2.606, 3.73)	(0.9618, 2.1217, 1.638, 3.22)	(0.9301, 2.1549, 2.058, 5.46)	(0.9052, 2.1549, 2.058, 5.46)	(0.9052, 2.1549, 2.058, 5.46)	(0.8943, 1.8487, 1.124, 1.68)			
0.90	(0.8555, 2.2241, 29.19)	(0.9859, 2.2678, 4.177, 13.60)	(0.9705, 2.2678, 4.177, 13.60)	(0.9618, 2.3417, 1.863, 16.91)	(0.9301, 2.2433, 2.897, 20.65)	(0.9052, 2.2433, 2.897, 20.65)	(0.9052, 2.2433, 2.897, 20.65)	(0.8943, 1.8487, 1.124, 1.68)			
1.10	(0.8574, 2.4895, 30.13)	(0.9859, 2.7462, 3.232, 15.48)	(0.9705, 2.7462, 3.232, 15.48)	(0.9618, 2.8217, 1.827, 18.58)	(0.9301, 2.7044, 2.359, 22.16)	(0.9052, 2.7044, 2.359, 22.16)	(0.9052, 2.7044, 2.359, 22.16)	(0.8943, 1.8487, 1.124, 1.68)			
1.25	(0.8604, 3.1876, 6.91)	(0.9915, 3.4337, 2.154, 3.92)	(0.9868, 3.3751, 1.815, 3.71)	(0.9688, 3.2712, 1.518, 3.64)	(0.9478, 3.2884, 1.761, 5.36)	(0.9237, 3.2420, 1.522, 5.18)	(0.9237, 3.2420, 1.522, 5.18)	(0.9033, 2.2779, 1.206, 20.87)			
1.50	(0.8294, 3.5389, 2.61)	(0.8511, 3.7536, 1.608, 2.82)	(0.7532, 3.7415, 1.520, 1.94)	(0.5428, 3.6780, 1.242, 1.74)	(0.6533, 3.7058, 1.437, 2.38)	(0.5892, 3.6706, 1.333, 2.27)	(0.5892, 3.6706, 1.333, 2.27)	(0.4770, 3.5851, 1.136, 2.13)			
0.50	(0.8354, 1.6809, 2.93)	(0.9928, 1.6103, 9.609, 9.94)	(0.9628, 1.6215, 1.766, 1.93)	(0.9255, 1.6922, 1.202, 1.34)	(0.8710, 1.7529, 1.619, 2.24)	(0.8569, 1.7598, 1.434, 2.05)	(0.8505, 1.7600, 1.237, 1.85)	(0.8432, 1.7720, 1.118, 1.74)			
0.75	(0.8496, 2.1802, 7.46)	(0.9928, 1.9732, 2.675, 3.93)	(0.9628, 1.9732, 2.675, 3.93)	(0.9549, 2.0513, 1.305, 3.84)	(0.9230, 2.0793, 2.126, 5.33)	(0.9001, 2.0793, 2.126, 5.33)	(0.8963, 2.0793, 2.126, 5.33)	(0.8843, 1.8487, 1.124, 1.68)			
0.90	(0.8535, 2.4201, 33.33)	(0.9928, 2.2024, 2.410, 14.94)	(0.9628, 2.2024, 2.410, 14.94)	(0.9549, 2.2805, 1.305, 3.84)	(0.9230, 2.2590, 2.808, 19.35)	(0.9001, 2.2590, 2.808, 19.35)	(0.9001, 2.2590, 2.808, 19.35)	(0.8843, 1.8487, 1.124, 1.68)			
1.10	(0.8574, 2.4895, 30.13)	(0.9928, 2.7462, 3.232, 15.48)	(0.9628, 2.7462, 3.232, 15.48)	(0.9549, 2.8217, 1.827, 18.58)	(0.9230, 2.7044, 2.359, 22.16)	(0.9001, 2.7044, 2.359, 22.16)	(0.9001, 2.7044, 2.359, 22.16)	(0.8843, 1.8487, 1.124, 1.68)			
1.25	(0.8604, 3.1876, 6.91)	(0.9915, 3.4337, 2.154, 3.92)	(0.9868, 3.3751, 1.815, 3.71)	(0.9688, 3.2712, 1.518, 3.64)	(0.9478, 3.2884, 1.761, 5.36)	(0.9237, 3.2420, 1.522, 5.18)	(0.9237, 3.2420, 1.522, 5.18)	(0.9033, 2.2779, 1.206, 20.87)			
1.50	(0.8294, 3.5389, 2.61)	(0.8511, 3.7536, 1.608, 2.82)	(0.7532, 3.7415, 1.520, 1.94)	(0.5428, 3.6780, 1.242, 1.74)	(0.6533, 3.7058, 1.437, 2.38)	(0.5892, 3.6706, 1.333, 2.27)	(0.5892, 3.6706, 1.333, 2.27)	(0.4770, 3.5851, 1.136, 2.13)			

Table 4: The parameters $\lambda^-, K_D, h_L, ATS_1$ and $\lambda^+, K_U, h_L, ATS_1$ of the VSI EWMA- γ^2 control charts compared with those λ^-, K_D, ARL_1 and λ^+, K_U, ARL_1 of FSI EWMA charts (second column) for $p = 3, n = 15, \gamma_0 = \{0.1, 0.2, 0.3, 0.4, 0.5\}$, $\tau = \{0.5, 0.75, 0.9, 1.1, 1.25, 1.5\}$ and $ATS_0 = 370.4$.

τ	FSI	$h_S=0.1$						$h_S=0.5$					
		$W=0.1$		$W=0.3$		$W=0.6$		$W=0.3$		$W=0.6$		$W=0.9$	
0.50	(0.1719, 1.6614, 14.27)	(0.2753, 1.4611, 2.919, 5.49)	(0.2441, 1.5173, 1.758, 6.08)	(0.1967, 1.6098, 1.396, 7.08)	(0.2048, 1.5933, 2.875, 8.88)	(0.2004, 1.5270, 1.423, 10.17)	(0.1888, 1.5591, 1.158, 10.75)						
0.75	(0.0442, 1.8912, 40.43)	(0.0309, 1.4019, 3.850, 5.94)	(0.2272, 1.4424, 2.953, 5.57)	(0.2470, 1.4880, 1.716, 6.17)	(0.1975, 1.5841, 1.296, 7.23)	(0.2051, 1.5688, 2.897, 10.01)	(0.1849, 1.6098, 1.168, 10.46)						
0.90	(0.0189, 1.6597, 111.22)	(0.0083, 1.8798, 3.053, 18.98)	(0.0638, 1.8798, 3.053, 18.98)	(0.0638, 1.8798, 3.053, 18.98)	(0.0638, 1.8798, 3.053, 18.98)	(0.0526, 1.8860, 1.455, 29.75)	(0.0508, 1.8882, 1.198, 31.42)						
1.10	(0.0087, 1.7855, 100.88)	(0.0135, 1.7251, 2.916, 7.17)	(0.0135, 1.7251, 2.916, 7.17)	(0.0135, 1.7251, 2.916, 7.17)	(0.0135, 1.7251, 2.916, 7.17)	(0.0129, 1.7860, 1.366, 93.77)	(0.0137, 1.7219, 1.195, 98.72)						
1.25	(0.0278, 2.8757, 384.63)	(0.0029, 2.0002, 3.525, 69.45)	(0.0029, 2.0002, 3.525, 69.45)	(0.0029, 2.0002, 3.525, 69.45)	(0.0029, 2.0002, 3.525, 69.45)	(0.0126, 1.7276, 4.478, 87.70)	(0.0130, 1.7146, 1.368, 97.10)						
1.50	(0.0710, 3.1572, 15.33)	(0.0441, 2.7952, 2.814, 22.62)	(0.0441, 2.7952, 2.814, 22.62)	(0.0441, 2.7952, 2.814, 22.62)	(0.0441, 2.7952, 2.814, 22.62)	(0.0111, 1.9143, 1.268, 87.78)	(0.0148, 2.0848, 1.131, 91.41)						
$\gamma_0 = 0.2$								(0.0329, 2.5885, 1.300, 30.07)	(0.0329, 2.5885, 1.300, 30.07)	(0.0329, 2.5885, 1.300, 30.07)	(0.0329, 2.5885, 1.300, 30.07)	(0.0319, 2.5716, 1.156, 12.51)	(0.0791, 3.2461, 1.157, 12.51)
0.50	(0.1727, 1.6357, 14.45)	(0.3112, 1.3777, 3.894, 6.03)	(0.2722, 1.4424, 2.953, 5.57)	(0.2470, 1.4880, 1.716, 6.17)	(0.1975, 1.5841, 1.296, 7.23)	(0.2004, 1.5270, 1.423, 10.17)	(0.1888, 1.5591, 1.158, 10.75)						
0.75	(0.0442, 1.8912, 40.43)	(0.0690, 1.8644, 5.242, 18.00)	(0.0690, 1.8644, 5.242, 18.00)	(0.0690, 1.8644, 5.242, 18.00)	(0.0690, 1.8644, 5.242, 18.00)	(0.0526, 1.8860, 1.455, 29.75)	(0.0508, 1.8882, 1.198, 31.42)						
0.90	(0.0189, 1.6597, 111.22)	(0.0135, 1.7502, 2.745, 67.52)	(0.0135, 1.7502, 2.745, 67.52)	(0.0135, 1.7502, 2.745, 67.52)	(0.0135, 1.7502, 2.745, 67.52)	(0.0129, 1.7860, 1.366, 93.77)	(0.0137, 1.7219, 1.195, 98.72)						
1.10	(0.0087, 1.7855, 100.88)	(0.0029, 2.0002, 3.525, 69.45)	(0.0029, 2.0002, 3.525, 69.45)	(0.0029, 2.0002, 3.525, 69.45)	(0.0029, 2.0002, 3.525, 69.45)	(0.0126, 1.7276, 4.478, 87.70)	(0.0130, 1.7146, 1.368, 97.10)						
1.25	(0.0278, 2.8757, 384.63)	(0.0421, 2.7754, 2.830, 24.38)	(0.0421, 2.7754, 2.830, 24.38)	(0.0421, 2.7754, 2.830, 24.38)	(0.0421, 2.7754, 2.830, 24.38)	(0.0126, 1.7276, 4.478, 87.70)	(0.0130, 1.7146, 1.368, 97.10)						
1.50	(0.0648, 3.1055, 16.24)	(0.1181, 3.6378, 2.241, 9.88)	(0.0993, 3.4739, 1.853, 9.75)	(0.0900, 3.3848, 1.474, 10.00)	(0.0788, 3.2464, 1.278, 10.57)	(0.0940, 3.4237, 1.771, 12.81)	(0.0679, 3.1434, 1.155, 13.10)						
$\gamma_0 = 0.3$								(0.0353, 3.2255, 1.485, 12.13)	(0.0353, 3.2255, 1.485, 12.13)	(0.0353, 3.2255, 1.485, 12.13)	(0.0353, 3.2255, 1.485, 12.13)	(0.0207, 1.5735, 1.427, 9.94)	(0.0542, 1.8860, 1.455, 29.75)
0.50	(0.1679, 1.6096, 14.75)	(0.3025, 1.3528, 4.005, 6.18)	(0.2741, 1.3994, 2.941, 5.70)	(0.2450, 1.4507, 1.738, 6.32)	(0.2006, 1.5340, 1.278, 7.49)	(0.2046, 1.5270, 1.423, 10.17)	(0.1888, 1.5591, 1.158, 10.75)						
0.75	(0.0451, 1.8590, 41.54)	(0.0683, 1.8287, 6.108, 18.74)	(0.0683, 1.8287, 6.108, 18.74)	(0.0683, 1.8287, 6.108, 18.74)	(0.0683, 1.8287, 6.108, 18.74)	(0.0522, 1.8826, 2.179, 29.51)	(0.0504, 1.8566, 1.193, 32.44)						
0.90	(0.0115, 1.6554, 113.88)	(0.0157, 1.7363, 7.382, 69.83)	(0.0157, 1.7363, 7.382, 69.83)	(0.0157, 1.7363, 7.382, 69.83)	(0.0157, 1.7363, 7.382, 69.83)	(0.0131, 1.6937, 4.853, 89.53)	(0.0147, 1.7218, 1.157, 101.40)						
1.10	(0.0082, 1.7257, 105.88)	(0.0099, 1.8438, 3.288, 74.11)	(0.0128, 2.0005, 2.135, 76.95)	(0.0135, 2.0324, 1.478, 81.13)	(0.0120, 1.9610, 1.291, 90.02)	(0.0090, 1.7854, 1.579, 89.90)	(0.0113, 1.9228, 1.113, 97.27)						
1.25	(0.0235, 2.5107, 40.83)	(0.0380, 2.7187, 2.823, 24.71)	(0.0341, 2.6406, 2.051, 25.06)	(0.0317, 2.5884, 1.531, 36.73)	(0.0341, 2.6406, 2.051, 25.06)	(0.0282, 2.9038, 1.589, 33.04)	(0.0276, 2.4915, 1.283, 33.04)						
1.50	(0.0597, 3.0125, 17.97)	(0.1047, 3.5703, 2.275, 10.39)	(0.0853, 3.3385, 1.831, 10.48)	(0.0712, 3.2189, 1.476, 10.79)	(0.0632, 3.1432, 1.270, 11.48)	(0.0714, 3.2222, 1.494, 13.08)	(0.0601, 3.0882, 1.268, 13.84)						
$\gamma_0 = 0.5$								(0.0212, 1.4728, 2.186, 10.20)	(0.0212, 1.4728, 2.186, 10.20)	(0.0212, 1.4728, 2.186, 10.20)	(0.0212, 1.4728, 2.186, 10.20)	(0.1819, 1.5115, 1.145, 11.19)	(0.2060, 1.4611, 1.405, 10.52)
0.50	(0.1684, 1.5442, 15.19)	(0.3030, 1.2955, 4.048, 6.36)	(0.2743, 1.3398, 2.948, 5.89)	(0.2488, 1.4104, 1.728, 6.50)	(0.1980, 1.4888, 1.255, 7.94)	(0.2041, 1.4666, 2.885, 10.53)	(0.1819, 1.5115, 1.145, 11.19)						
0.75	(0.0489, 1.8073, 43.14)	(0.0673, 1.7708, 6.354, 19.70)	(0.0693, 1.7839, 3.200, 20.60)	(0.0605, 1.7845, 1.799, 23.01)	(0.0532, 1.7963, 1.329, 26.02)	(0.0537, 1.7955, 4.137, 30.32)	(0.0513, 1.7994, 1.438, 32.06)						
0.90	(0.0123, 1.6386, 117.81)	(0.0152, 1.6985, 7.611, 73.29)	(0.0148, 1.6924, 3.018, 77.48)	(0.0163, 1.7143, 1.721, 85.41)	(0.0171, 1.7217, 1.289, 95.07)	(0.0148, 1.6923, 4.070, 93.16)	(0.0148, 1.6923, 1.151, 105.40)						
1.10	(0.0059, 1.5471, 111.48)	(0.0094, 1.7975, 3.550, 78.68)	(0.0124, 1.9710, 1.437, 88.94)	(0.0124, 1.9710, 1.437, 88.94)	(0.0130, 2.0001, 1.202, 96.11)	(0.0087, 1.7566, 2.283, 93.39)	(0.0081, 1.7170, 1.217, 99.33)						
1.25	(0.0201, 2.2797, 44.47)	(0.0331, 2.6280, 2.835, 26.87)	(0.0336, 2.6410, 2.000, 27.43)	(0.0241, 2.4015, 1.479, 29.48)	(0.0336, 2.6403, 1.251, 32.29)	(0.0267, 2.4744, 2.092, 34.80)	(0.0240, 2.4004, 1.266, 36.12)						
1.50	(0.0445, 2.5560, 19.73)	(0.0871, 3.4518, 2.382, 11.71)	(0.0713, 3.2609, 1.837, 11.64)	(0.0548, 3.0278, 1.446, 12.48)	(0.0560, 3.0465, 1.255, 12.88)	(0.0626, 3.1427, 1.786, 15.07)	(0.0504, 2.9574, 1.258, 15.55)						
$\gamma_0 = 0.5$								(0.1894, 1.3895, 1.381, 11.01)	(0.1894, 1.3895, 1.381, 11.01)	(0.1894, 1.3895, 1.381, 11.01)	(0.1894, 1.3895, 1.381, 11.01)	(0.1701, 1.4453, 1.197, 11.76)	(0.1701, 1.4453, 1.197, 11.76)
0.50	(0.1649, 1.5727, 15.77)	(0.3063, 1.2909, 4.509, 6.65)	(0.2752, 1.3353, 1.659, 6.05)	(0.2490, 1.4143, 1.704, 6.43)	(0.1980, 1.4888, 1.255, 7.94)	(0.2041, 1.4666, 2.885, 10.53)	(0.1819, 1.5115, 1.145, 11.19)						
0.75	(0.0442, 1.8257, 45.33)	(0.0663, 1.8855, 6.347, 21.00)	(0.0624, 1.8798, 3.108, 21.90)	(0.0630, 1.7136, 1.294, 28.57)	(0.0532, 1.7963, 1.329, 26.02)	(0.0537, 1.7955, 4.137, 30.32)	(0.0513, 1.7994, 1.438, 32.06)						
0.90	(0.0128, 1.5965, 123.12)	(0.0175, 1.6672, 6.702, 78.51)	(0.0148, 1.6296, 1.674, 90.88)	(0.0172, 1.6639, 1.273, 100.87)	(0.0128, 1.5965, 1.193, 105.40)	(0.0148, 1.6296, 4.070, 93.16)	(0.0148, 1.6296, 1.151, 105.40)						
1.10	(0.0043, 1.3195, 119.49)	(0.0081, 1.6945, 3.119, 85.24)	(0.0081, 1.6945, 3.119, 85.24)	(0.0092, 1.7612, 1.374, 97.90)	(0.0128, 1.9610, 1.291, 90.02)	(0.0056, 1.4673, 2.119, 100.02)	(0.0081, 1.7146, 1.202, 107.64)						
1.25	(0.0146, 2.0411, 49.67)	(0.0274, 2.2701, 2.832, 30.02)	(0.0219, 2.3114, 1.945, 30.96)	(0.0197, 2.2888, 1.428, 33.66)	(0.0225, 2.3294, 1.212, 37.04)	(0.0210, 2.2837, 2.014, 38.96)	(0.0196, 2.2381, 1.238, 40.84)						
1.50	(0.0335, 2.6213, 23.08)	(0.0702, 3.2616, 2.375, 13.38)	(0.0557, 3.0438, 1.800, 13.44)	(0.0491, 2.9388, 1.427, 14.17)	(0.0413, 2.8760, 1.482, 17.82)	(0.0516, 2.9773, 1.796, 17.87)	(0.0424, 2.8090, 1.239, 18.19)						

Table 5: The parameters $\lambda^-, K_D, h_L, ATS_1$ and $\lambda^+, K_U, h_L, ATS_1$ of the VSI EWMA- γ^2 control charts compared with those λ^-, K_D, ARL_1 and λ^+, K_U, ARL_1 of FSI EWMA charts (second column) for $p = 4, n = 5, \gamma_0 = \{0.1, 0.2, 0.3, 0.4, 0.5\}, \tau = \{0.5, 0.75, 0.9, 1.1, 1.25, 1.5\}$ and $ATS_0 = 370.4$.

τ	FSI	$h_S=0.1$					$h_S=0.5$				
		$\gamma_0=0.1$	$W=0.3$	$W=0.6$	$W=0.9$	$W=1.0$	$\gamma_0=0.1$	$W=0.3$	$W=0.6$	$W=0.9$	$W=1.0$
0.50	(0.8209, 1.9272, 2.17)	(0.8300, 1.8559, 1.964, 2.12)	(0.8539, 2.2758, 2.724, 3.14)	(0.8698, 1.8863, 1.416, 1.54)	(0.8698, 1.8867, 1.210, 1.34)	(0.8692, 1.9065, 1.578, 2.17)	(0.8530, 2.2758, 1.957, 3.97)	(0.8330, 1.8282, 1.439, 1.91)	(0.8530, 1.9201, 1.247, 1.84)	(0.8506, 1.9223, 1.126, 1.72)	
0.75	(0.8268, 2.2988, 7.69)	(0.8268, 2.2988, 7.69)	(0.8268, 2.2988, 7.69)	(0.8268, 2.2988, 7.69)	(0.8268, 2.2988, 7.69)	(0.8268, 2.2988, 7.69)	(0.8268, 2.2988, 7.69)	(0.8268, 2.2988, 7.69)	(0.8268, 2.2988, 7.69)	(0.8268, 2.2988, 7.69)	
0.90	(0.8487, 2.2883, 26.95)	(0.8487, 2.2883, 26.95)	(0.8487, 2.2883, 26.95)	(0.8487, 2.2883, 26.95)	(0.8487, 2.2883, 26.95)	(0.8487, 2.2883, 26.95)	(0.8487, 2.2883, 26.95)	(0.8487, 2.2883, 26.95)	(0.8487, 2.2883, 26.95)	(0.8487, 2.2883, 26.95)	
1.10	(0.8480, 2.5681, 26.53)	(0.8480, 2.5681, 26.53)	(0.8480, 2.5681, 26.53)	(0.8480, 2.5681, 26.53)	(0.8480, 2.5681, 26.53)	(0.8480, 2.5681, 26.53)	(0.8480, 2.5681, 26.53)	(0.8480, 2.5681, 26.53)	(0.8480, 2.5681, 26.53)	(0.8480, 2.5681, 26.53)	
1.25	(0.1664, 3.1262, 7.37)	(0.1664, 3.1262, 7.37)	(0.1664, 3.1262, 7.37)	(0.1664, 3.1262, 7.37)	(0.1664, 3.1262, 7.37)	(0.1664, 3.1262, 7.37)	(0.1664, 3.1262, 7.37)	(0.1664, 3.1262, 7.37)	(0.1664, 3.1262, 7.37)	(0.1664, 3.1262, 7.37)	
1.50	(0.4028, 3.5395, 2.78)	(0.4028, 3.5395, 2.78)	(0.4028, 3.5395, 2.78)	(0.4028, 3.5395, 2.78)	(0.4028, 3.5395, 2.78)	(0.4028, 3.5395, 2.78)	(0.4028, 3.5395, 2.78)	(0.4028, 3.5395, 2.78)	(0.4028, 3.5395, 2.78)	(0.4028, 3.5395, 2.78)	
0.50	(0.8131, 1.8987, 2.23)	(0.8131, 1.8987, 2.23)	(0.8131, 1.8987, 2.23)	(0.8131, 1.8987, 2.23)	(0.8131, 1.8987, 2.23)	(0.8131, 1.8987, 2.23)	(0.8131, 1.8987, 2.23)	(0.8131, 1.8987, 2.23)	(0.8131, 1.8987, 2.23)	(0.8131, 1.8987, 2.23)	
0.75	(0.8268, 2.2988, 7.69)	(0.8268, 2.2988, 7.69)	(0.8268, 2.2988, 7.69)	(0.8268, 2.2988, 7.69)	(0.8268, 2.2988, 7.69)	(0.8268, 2.2988, 7.69)	(0.8268, 2.2988, 7.69)	(0.8268, 2.2988, 7.69)	(0.8268, 2.2988, 7.69)	(0.8268, 2.2988, 7.69)	
0.90	(0.8487, 2.2883, 26.95)	(0.8487, 2.2883, 26.95)	(0.8487, 2.2883, 26.95)	(0.8487, 2.2883, 26.95)	(0.8487, 2.2883, 26.95)	(0.8487, 2.2883, 26.95)	(0.8487, 2.2883, 26.95)	(0.8487, 2.2883, 26.95)	(0.8487, 2.2883, 26.95)	(0.8487, 2.2883, 26.95)	
1.10	(0.8480, 2.5681, 26.53)	(0.8480, 2.5681, 26.53)	(0.8480, 2.5681, 26.53)	(0.8480, 2.5681, 26.53)	(0.8480, 2.5681, 26.53)	(0.8480, 2.5681, 26.53)	(0.8480, 2.5681, 26.53)	(0.8480, 2.5681, 26.53)	(0.8480, 2.5681, 26.53)	(0.8480, 2.5681, 26.53)	
1.25	(0.1664, 3.1262, 7.37)	(0.1664, 3.1262, 7.37)	(0.1664, 3.1262, 7.37)	(0.1664, 3.1262, 7.37)	(0.1664, 3.1262, 7.37)	(0.1664, 3.1262, 7.37)	(0.1664, 3.1262, 7.37)	(0.1664, 3.1262, 7.37)	(0.1664, 3.1262, 7.37)	(0.1664, 3.1262, 7.37)	
1.50	(0.4028, 3.5395, 2.78)	(0.4028, 3.5395, 2.78)	(0.4028, 3.5395, 2.78)	(0.4028, 3.5395, 2.78)	(0.4028, 3.5395, 2.78)	(0.4028, 3.5395, 2.78)	(0.4028, 3.5395, 2.78)	(0.4028, 3.5395, 2.78)	(0.4028, 3.5395, 2.78)	(0.4028, 3.5395, 2.78)	

Table 6: The parameters $\lambda^-, K_D, h_L, AT S_1$ and $\lambda^+, K_U, h_L, AT S_1$ of the VSI EWMA- γ^2 control charts compared with those λ^-, K_D, ARL_1 and λ^+, K_U, ARL_1 of FSI EWMA charts (second column) for $p = 4, n = 15, \gamma_0 = \{0.1, 0.2, 0.3, 0.4, 0.5\}$, $\tau = \{0.5, 0.75, 0.9, 1.1, 1.25, 1.5\}$ and $AT S_0 = 370.4$.

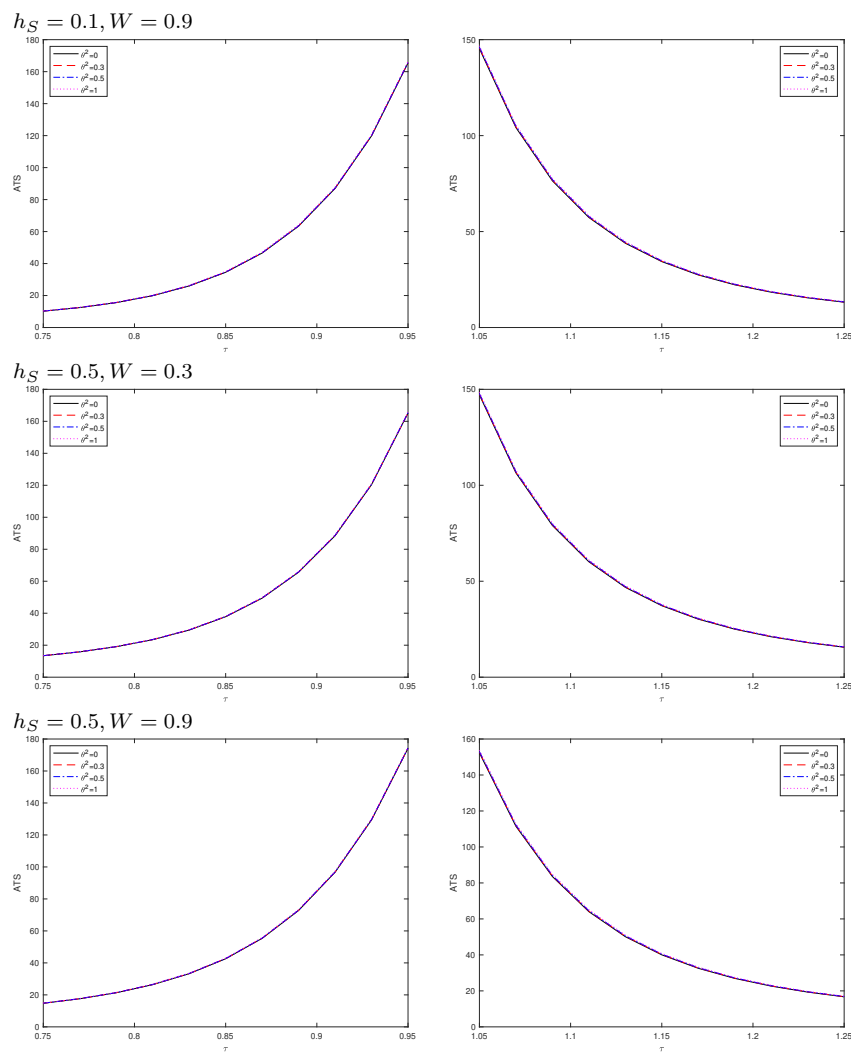


Fig. 10: ATS curves of the downward (left) and upward (right) VSI EWMA MCV charts for $p = 2, \gamma_0 = 0.1, n = 5$ with measurement parameters $B = 1, m = 1$, and $\theta^2 \in \{0, 0.3, 0.5, 1\}$.

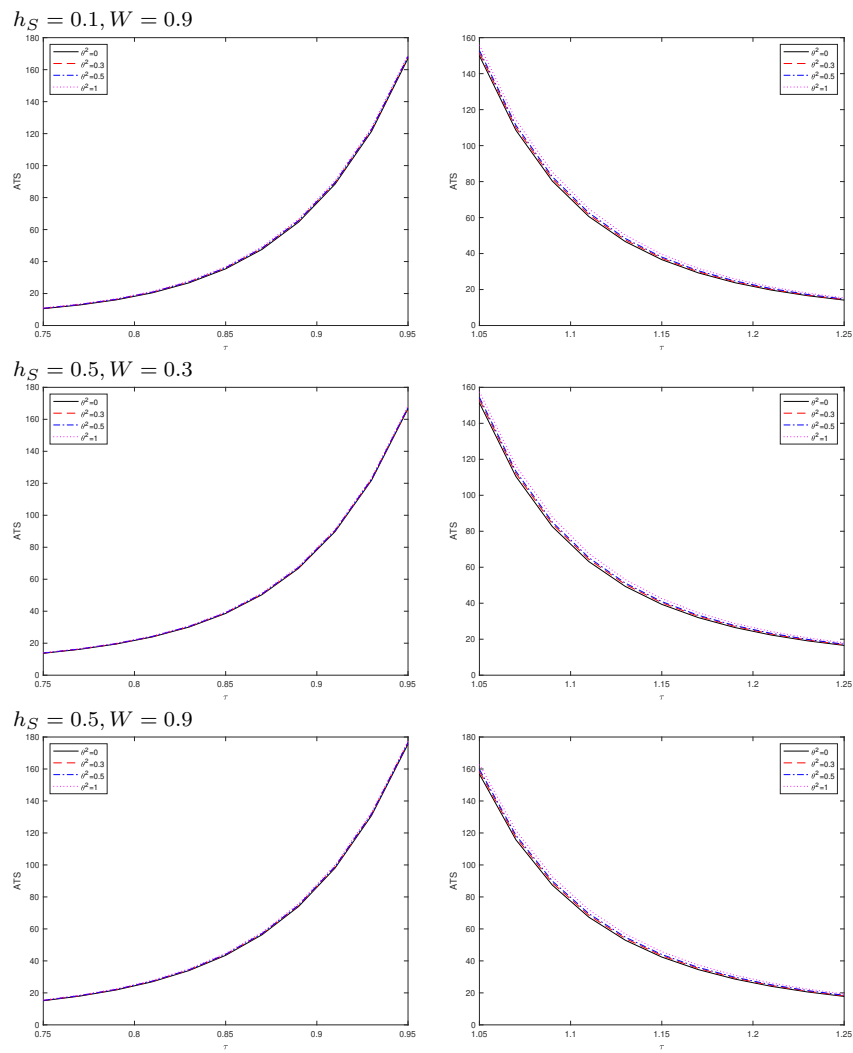


Fig. 11: ATS curves of the downward (left) and upward (right) VSI EWMA MCV charts for $p = 2, \gamma_0 = 0.2, n = 5$ with measurement parameters $B = 1, m = 1$, and $\theta^2 \in \{0, 0.3, 0.5, 1\}$.

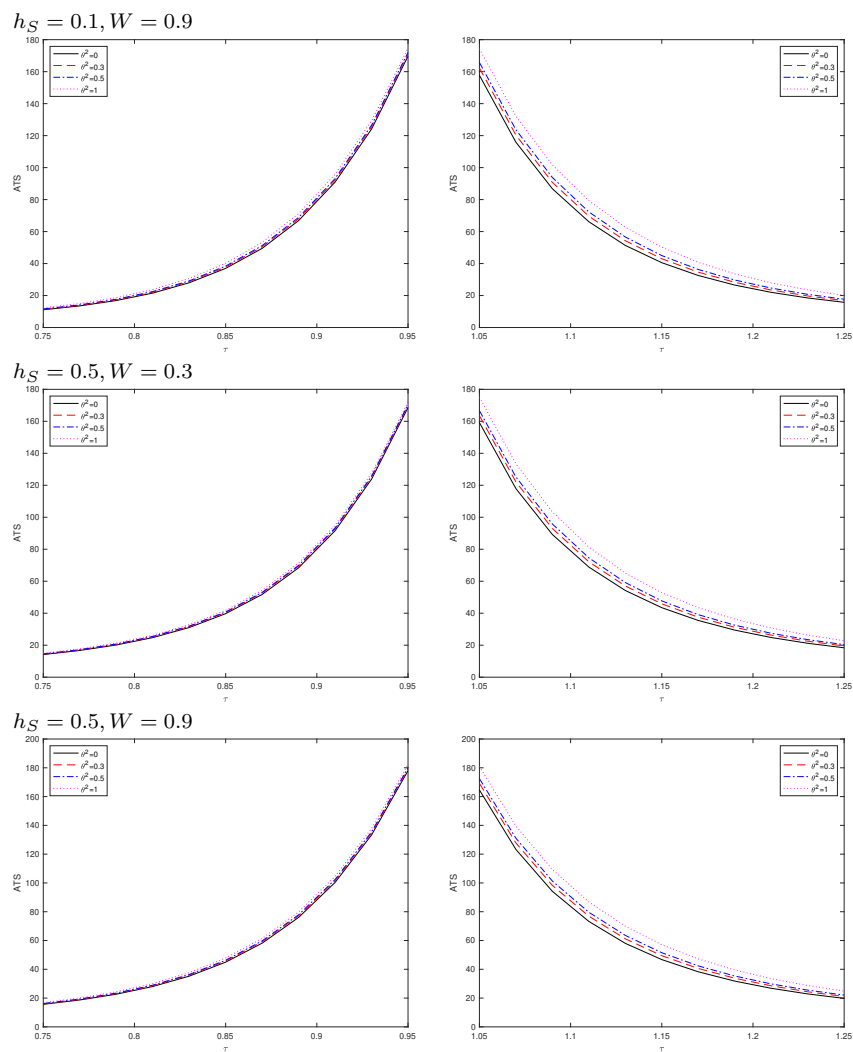


Fig. 12: ATS curves of the downward (left) and upward (right) VSI EWMA MCV charts for $p = 2, \gamma_0 = 0.3, n = 5$ with measurement parameters $B = 1, m = 1$, and $\theta^2 \in \{0, 0.3, 0.5, 1\}$.

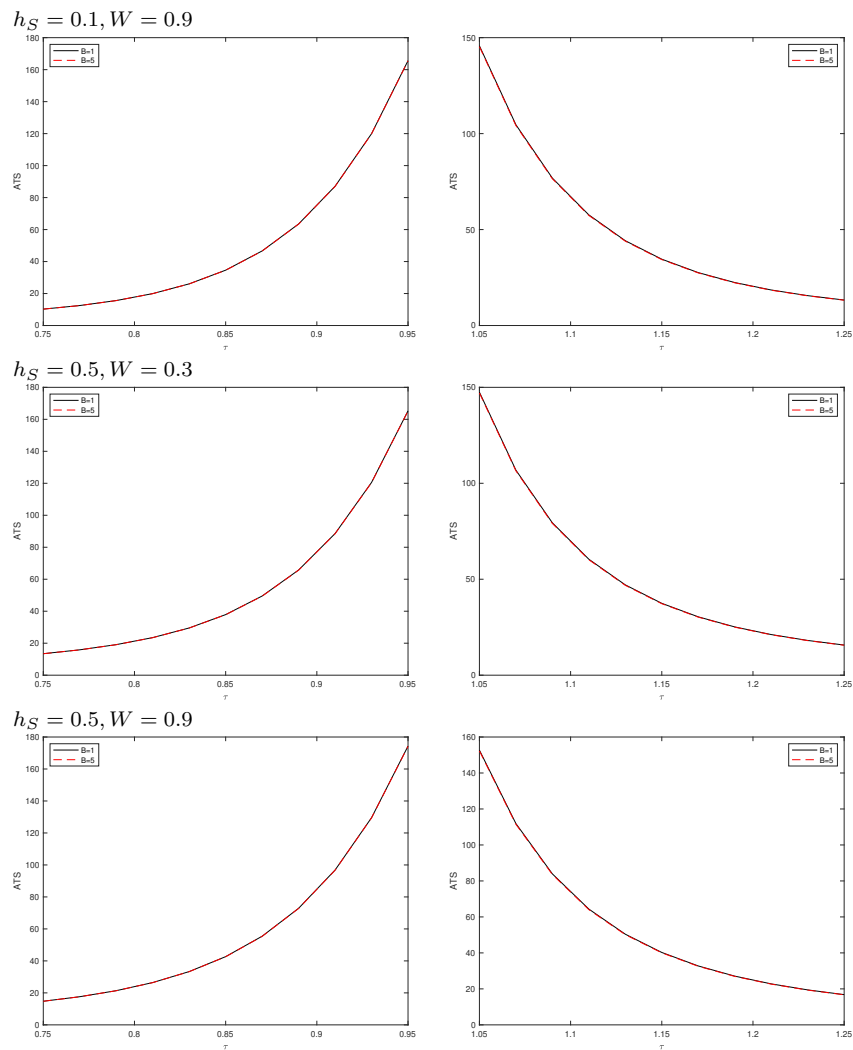


Fig. 13: ATS curves of the downward (left) and upward (right) VSI EWMA MCV charts for $p = 2$, $\gamma_0 = 0.1$, $n = 5$ with measurement parameters $\theta^2 = 0.3$, $m = 1$, and $B \in \{1, 5\}$.

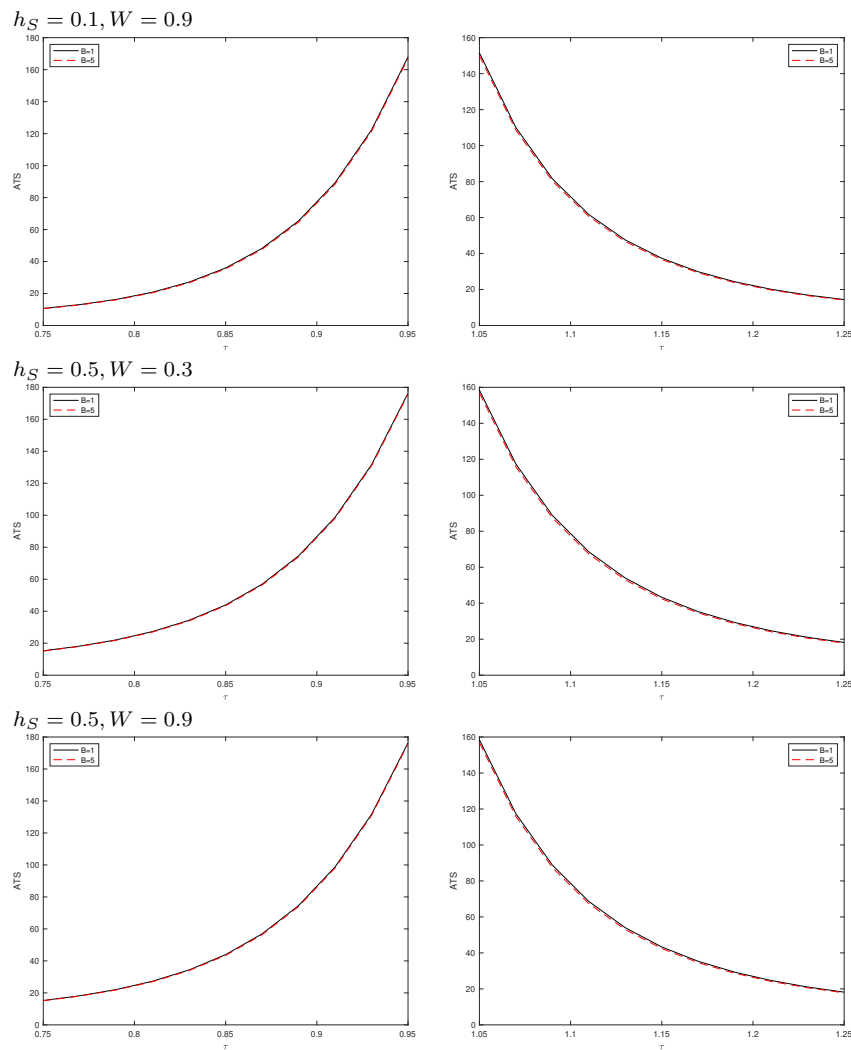


Fig. 14: ATS curves of the downward (left) and upward (right) VSI EWMA MCV charts for $p = 2, \gamma_0 = 0.2, n = 5$ with measurement parameters $\theta^2 = 0.3, m = 1$, and $B \in \{1, 5\}$.

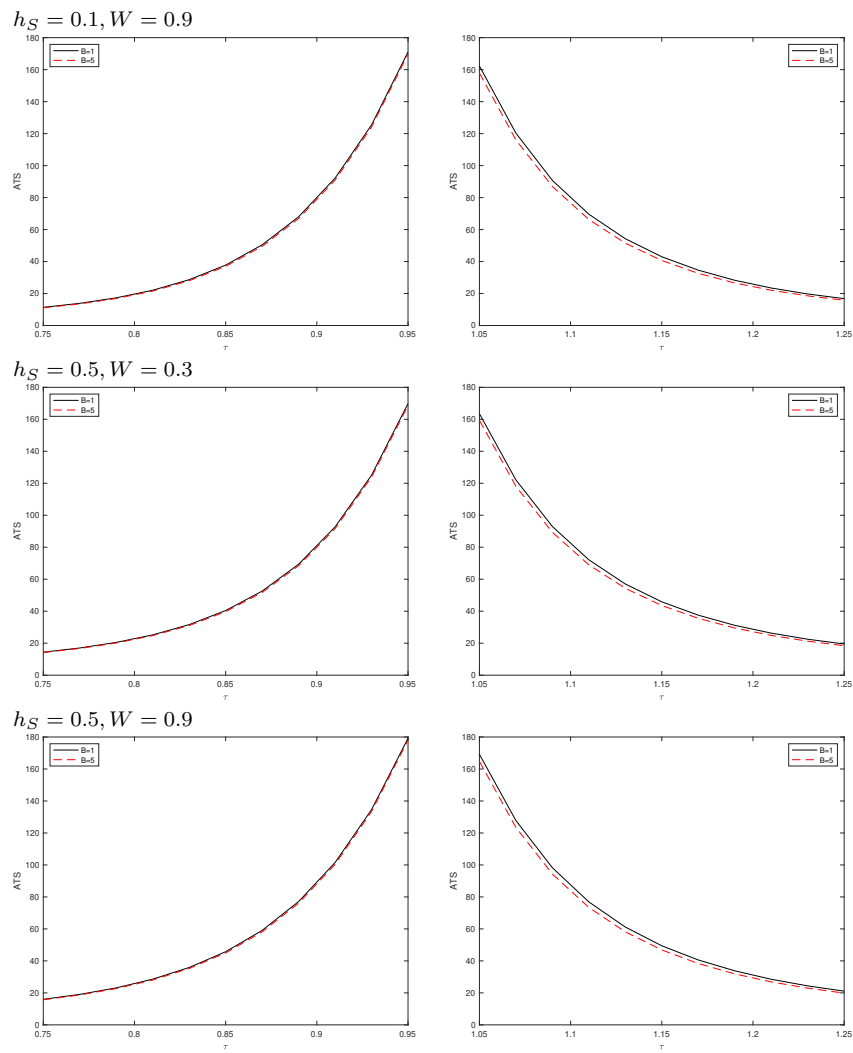


Fig. 15: ATS curves of the downward (left) and upward (right) VSI EWMA MCV charts for $p = 2$, $\gamma_0 = 0.3$, $n = 5$ with measurement parameters $\theta^2 = 0.3$, $m = 1$, and $B \in \{1, 5\}$.

p	τ	Syn MCV	VSSI MCV	VSI EWMA
$\gamma_0 = 0.1$				
2	1.25	27.08	16.99	10.04
	1.50	9.19	4.19	4.33
3	1.25	34.92	26.37	13.54
	1.50	12.40	6.28	5.71
$\gamma_0 = 0.3$				
2	1.25	30.18	20.88	10.99
	1.50	10.53	4.94	4.75
3	1.25	38.67	31.93	14.84
	1.50	14.20	7.55	6.32
$\gamma_0 = 0.5$				
2	1.25	37.77	30.62	13.47
	1.50	13.93	6.79	5.83
3	1.25	47.97	45.14	18.16
	1.50	18.92	10.81	7.89

Table 7: Comparison with the VSSI MCV control charts [22] and synthetic MCV [29], for different values of $n = 5$, $p = \{2, 3\}$, $\gamma_0 = \{0.1, 0.2, 0.3\}$, $ARL_0 = 370.4$ and upper shifts $\tau = \{1.25, 1.50\}$.

p	τ	$\gamma_0 = 0.1$		$\gamma_0 = 0.3$		$\gamma_0 = 0.5$	
		VSI EWMA	RS MCV	VSI EWMA	RS MCV	VSI EWMA	RS MCV
2	0.50	3.2	6.4	3.3	6.7	3.62	7.2
	0.75	7.9	28.9	8.4	30.7	9.51	34.7
	0.90	31.7	122.1	33.8	127.2	38.94	137.3
	1.10	34.5	88.3	37.2	94.4	44.87	108.2
	1.25	10.0	23.8	11.0	26.6	13.47	33.5
	1.50	4.3	7.8	4.8	8.9	5.82	11.9
3	0.50	3.9	9.6	4.1	10.0	4.4	10.7
	0.75	10.5	43.7	11.2	46.4	12.6	52.1
	0.90	42.1	153.8	44.7	159.3	50.8	169.7
	1.10	45.2	107.1	48.7	113.3	57.5	127.7
	1.25	13.5	32.3	14.8	35.9	18.2	44.9
	1.50	5.7	10.8	6.3	12.5	7.9	17.0

Table 8: Comparison with the run sum control charts, for different values of $n = 5$, $p = \{2, 3\}$, $\gamma_0 = \{0.1, 0.2, 0.3\}$, $\tau = \{0.5, 0.75, 0.9, 1.10, 1.25, 1.50\}$ and $ARL_0 = 370$.